Star formation

WS24/25

Protostellar evolution
&
Pre-main-sequence evolution

Caroline Gieser
gieser@mpia.de

Sternentstehung - Star Formation

Winter term 2024/2025

Henrik Beuther, Thomas Henning & Caroline Gieser

15.10 Today: Introduction & Overview (Beuther)
22.10 Physical processes I (Beuther)
29.10 --
05.11 Physcial processes II (Beuther)
12.11 Molecular clouds as birth places of stars (Beuther)
19.11 Molecular clouds (cont.), Jeans Analysis (Henning)
26.11 Collapse models I (Beuther)
03.12 Collapse models II (Beuther)
10.12 Protostellar evolution (Gieser)
17.12 Pre-main sequence evolution & outflows/jets (Henning)
07.01 Accretion disks I (Henning)
14.01 Accretion disks II (Henning)
21.01 High-mass star formation, clusters and the IMF (Gieser)
28.01 Extragalactic star formation (Henning)
04.02 Planetarium@HdA, outlook, questions (Beuther, Gieser, Henning)
11.02 Examination week, no star formation lecture

Book: Stahler & Palla: The Formation of Stars, Wileys

More Information and the current lecture files: http://www.mpia.de/homes/beuther/lecture_ws2425.html

beuther@mpia.de, henning@mpia.de , gieser@mpia.de

Large scale molecular cloud collapse

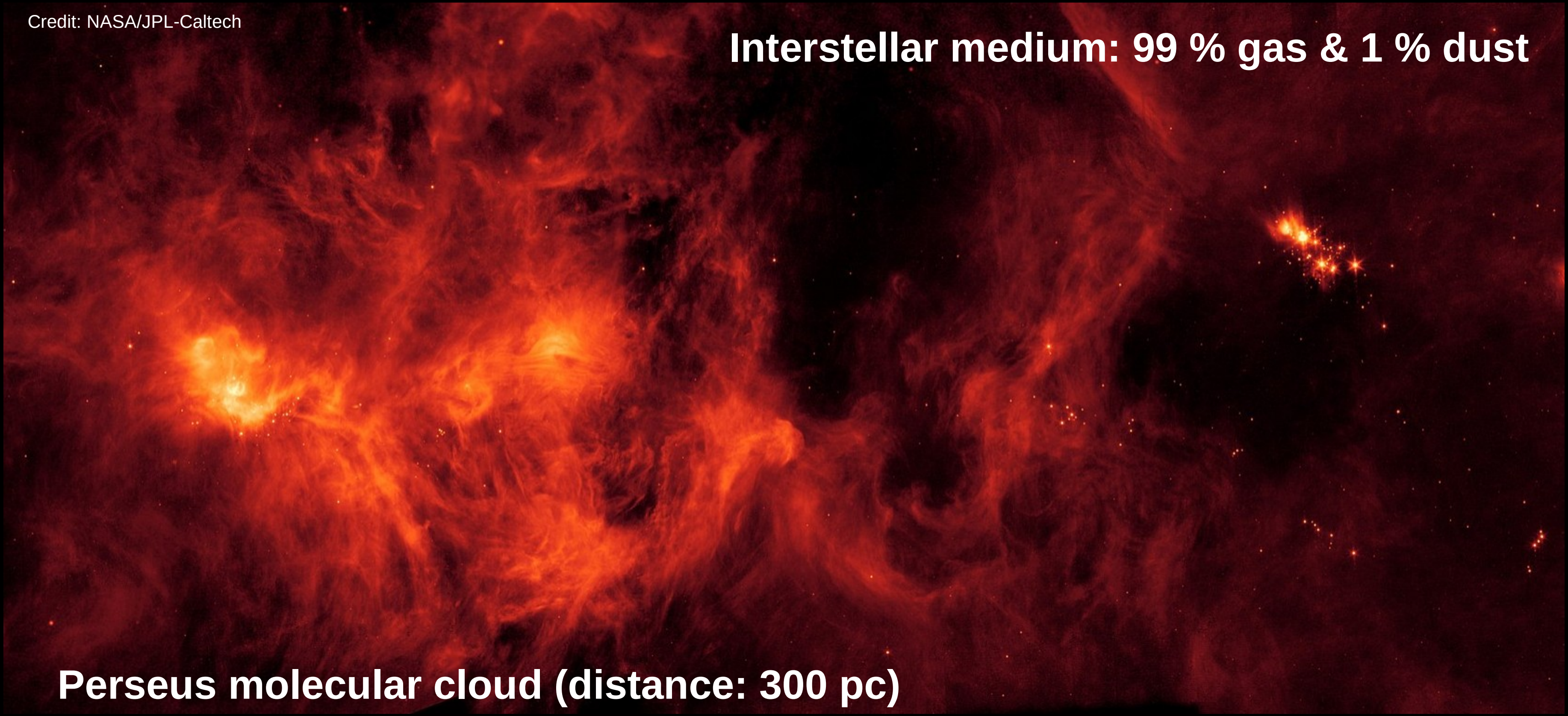

Spitzer space telescope: infrared

Zooming into star-forming regions

Pillars of creation

Hubble telescope: optical

James Webb space telescope (JWST): infrared

Young embdedded protostars

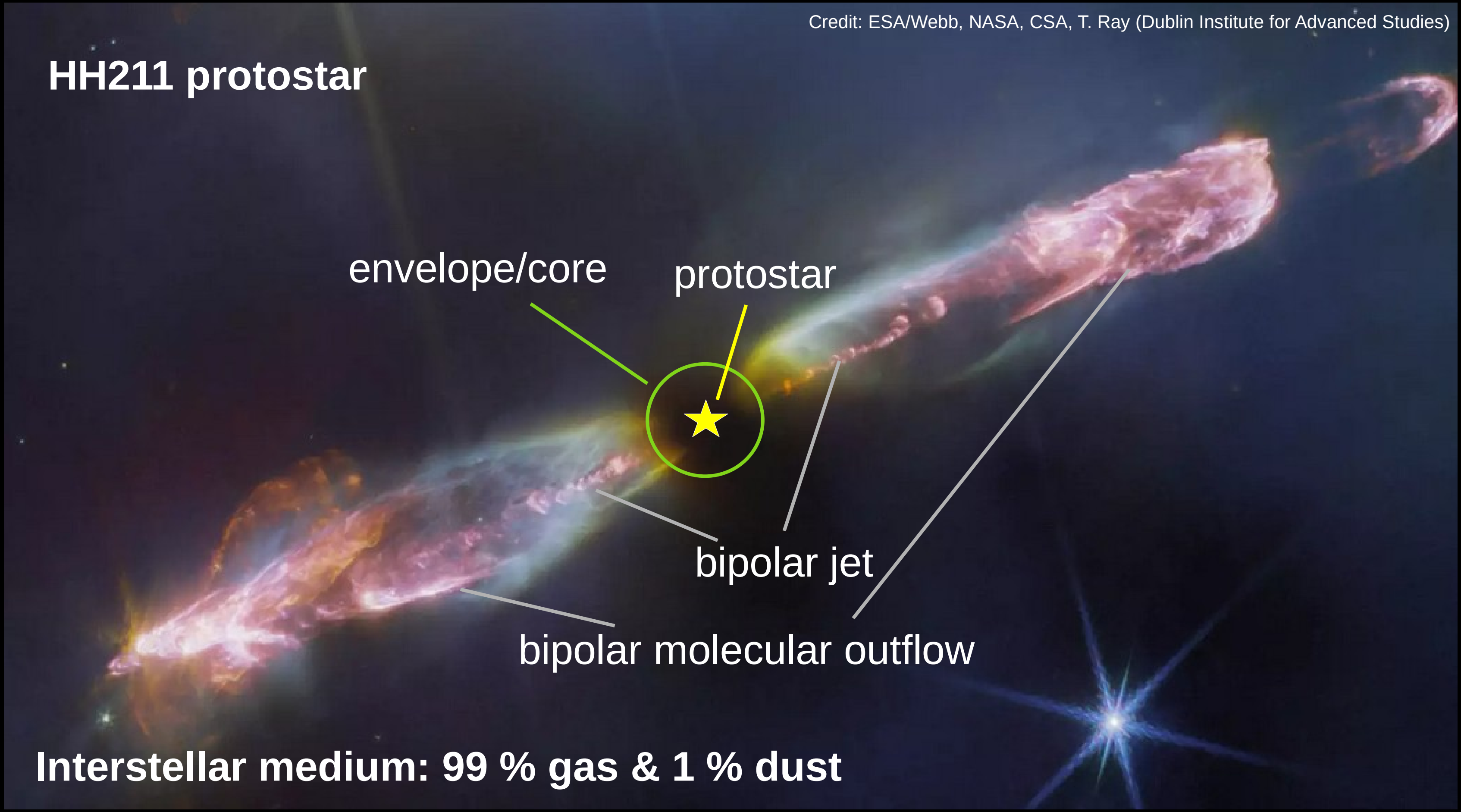

JWST: infrared

Topics today

- **The first core and accretion luminosity**
- The protostellar envelope
- Protostellar evolution
- Pre-main sequence evolution

Section 11.1 in Stahler & Palla

The first core

recap from previous lectures:

initial cloud and dense core collapse:
→ slow contraction
→ cooling via dust, atoms (C, O), molecules (CO)

forces to consider:
gravity ↔ thermal pressure (& magnetic field)

stability criterion: Jeans mass M_J

$$M_J = 1.0\ M_\odot \left(\frac{T}{10\ \mathrm{K}}\right)^{3/2} \left(\frac{n_{\mathrm{H_2}}}{10^4\ \mathrm{cm^{-3}}}\right)^{-1/2}$$

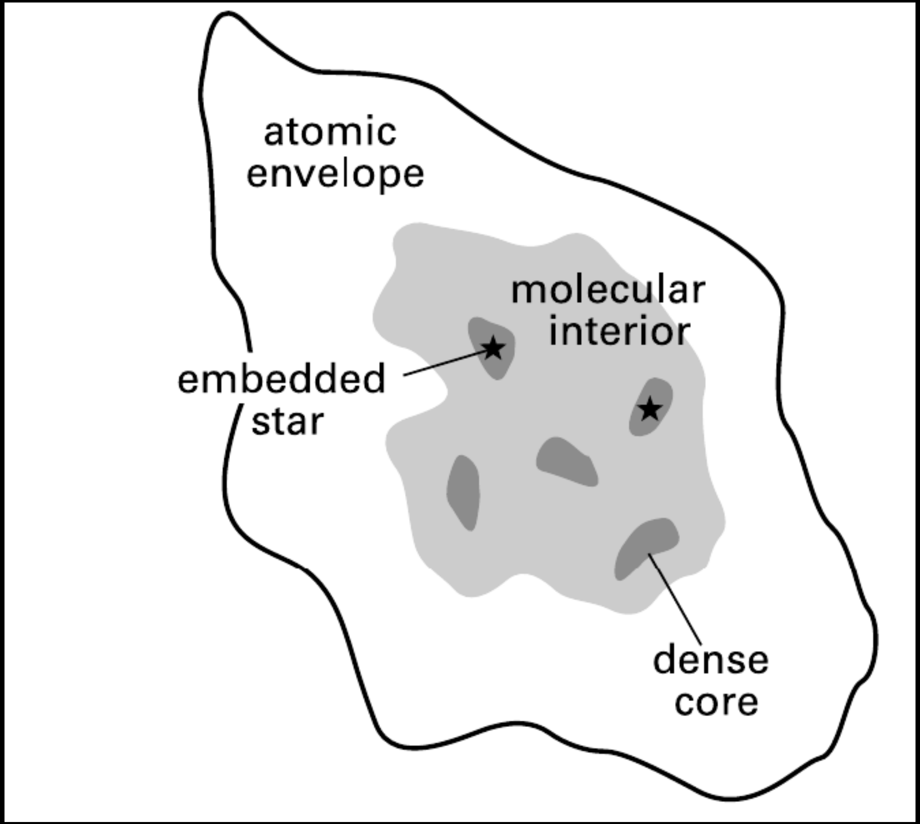

Fig. 8.1

The first core

recap from previous lectures:

ambipolar diffusion:
→ decoupling between ions and
neutral atoms and molecules

low ionization fraction in dense cores:
→ electrons and ions tied to magnetic field
→ neutral species further contract

→ density increases while magnetic support decreases
with time

Σ (mass surface density) / B (magnetic field) > critical value:
→ **contraction speeds up**

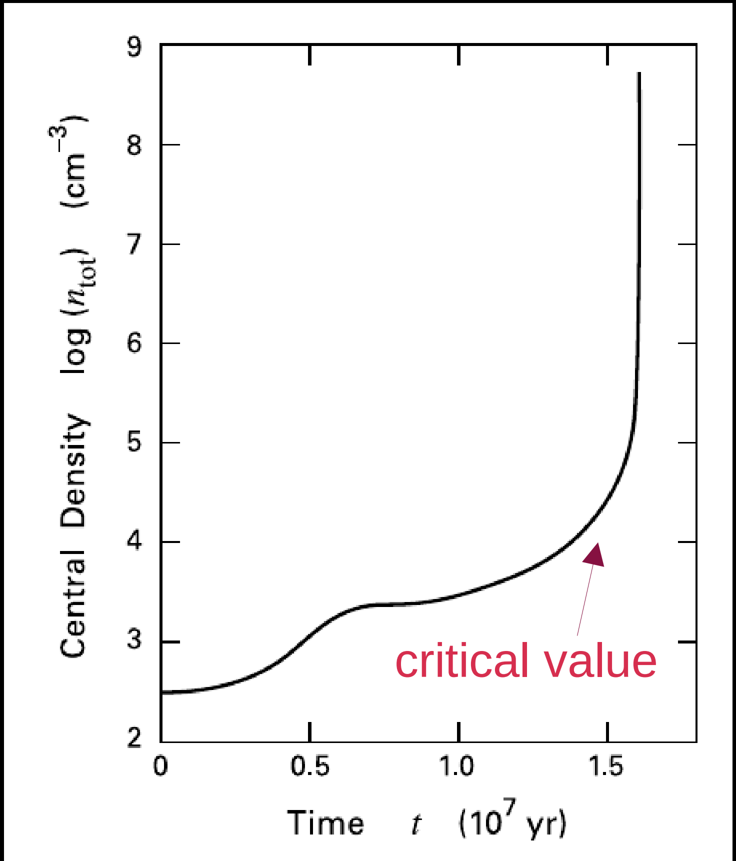

Fig. 10.4

The first core

virial theorem: $$2\mathcal{T} + 2U + \mathcal{W} + \mathcal{M} = 0$$

system in equilibrium

The first core

kinetic energy T = 0

magnetic energy M = 0

virial theorem: $$2\mathcal{T} + 2U + \mathcal{W} + \mathcal{M} = 0$$

The first core

kinetic energy T = 0

magnetic energy M = 0

virial theorem: $$2\mathcal{T} + 2U + \mathcal{W} + \mathcal{M} = 0$$

internal energy U

$$= \frac{3}{2}\frac{\mathcal{R}T}{\mu}M$$

potential energy W

$$= -GM^2/R,$$

$\mathcal{R}$: gas constant (N_A*k_B)
G: gravitational constant
μ: mean molecular weight
(μ=2.4 in molecular clouds)

***T*: core temperature**
***M*: core mass**
***R*: core radius**

→ What is the core temperature after collapse?

The first core

virial theorem: $$2\mathcal{T} + 2\mathcal{U} + \mathcal{W} + \mathcal{M} = 0$$

core temperature:
$$T \approx \frac{\mu}{3\mathcal{R}} \frac{GM}{R} = 850\ \mathrm{K} \left(\frac{M}{5 \times 10^{-2}\ M_{\odot}}\right) \left(\frac{R}{5\ \mathrm{AU}}\right)^{-1}$$

→ **significantly warmer than the natal cloud material (T~10K)**

The first core

(also Fig. 11.1)

molecular cloud and dense core collapse:
→ isothermal (T~10K)

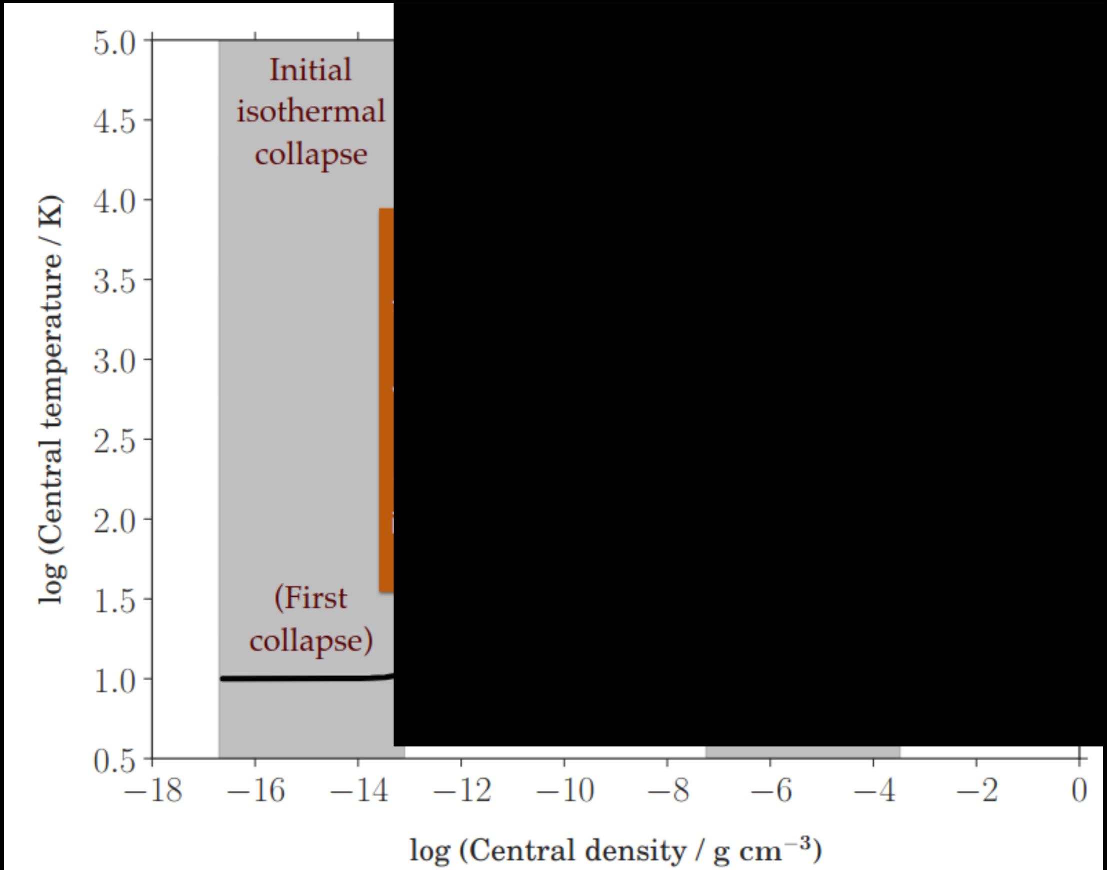

Bhandare et al., A&A 618, A95 (2018)

The first core

(also Fig. 11.1)

molecular cloud and dense core collapse:
→ isothermal (T~10K)

first core formation:
→ core becomes opaque
→ cooling less efficient
→ adiabatic process:
grav. potential energy heats the core
→ temperature and density increase

chemical composition:
→ still mostly molecular hydrogen (H_2)

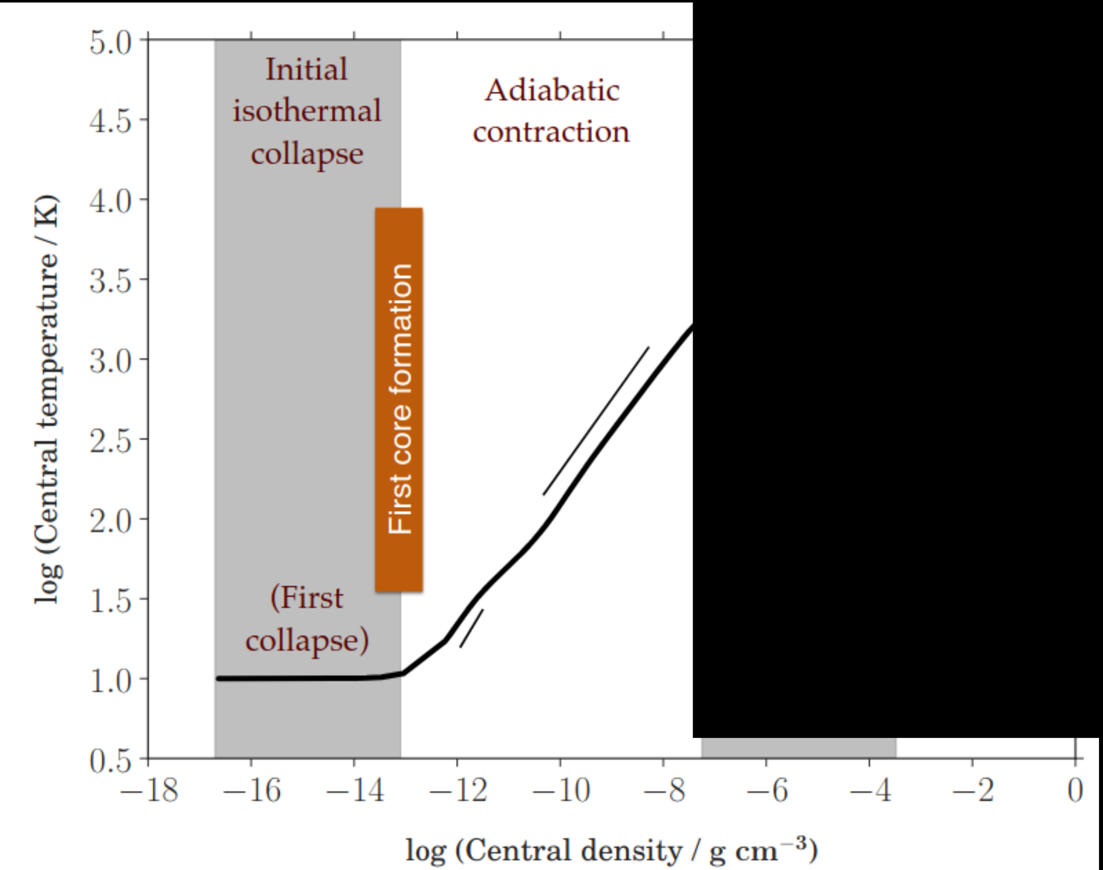

Bhandare et al., A&A 618, A95 (2018)

The first core

(also Fig. 11.1)

second collapse:

→ collisional dissociation of H_2 at T=2000K

→ dissociated H_2 absorbs most of gravitational potential energy

→ moderate increase of temperature and density

center: atomic hydrogen zone that spreads outwards

envelope: H_2

→ first core collapses and a **protostar** is born

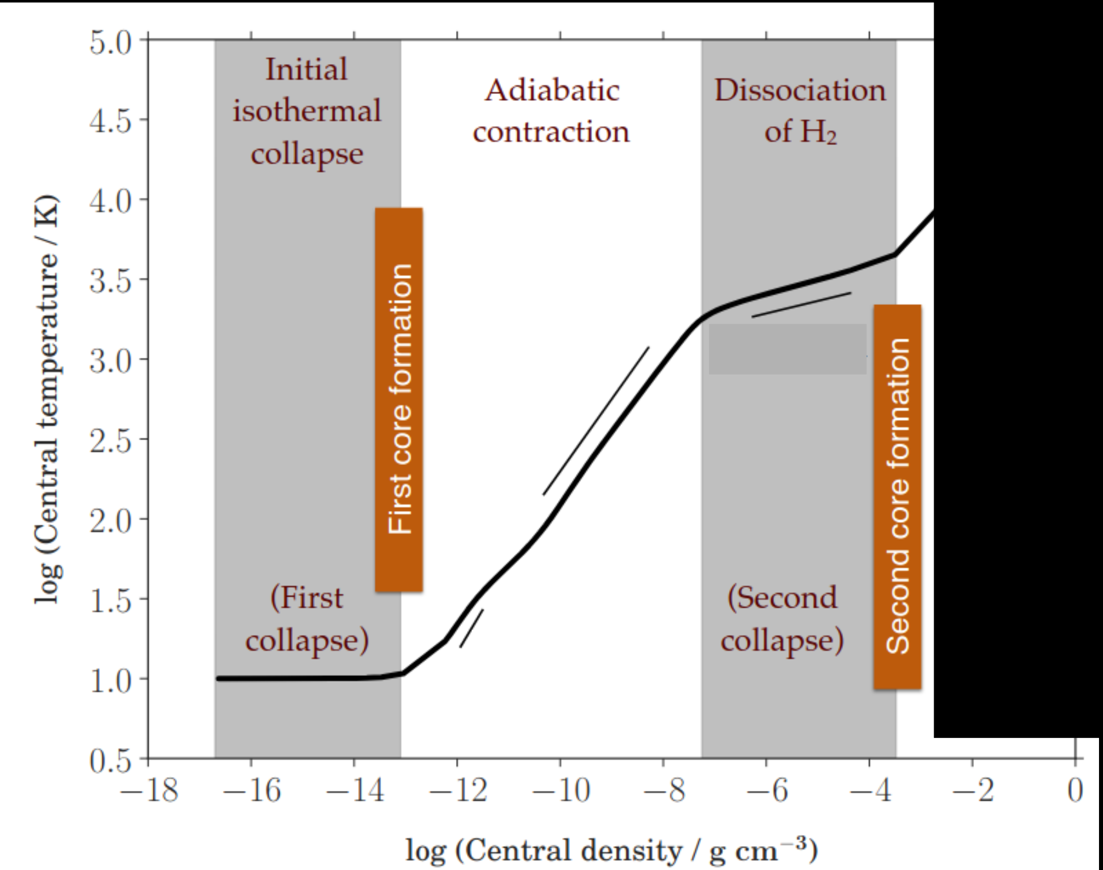

Bhandare et al., A&A 618, A95 (2018)

The first core

(also Fig. 11.1)

protostar:

→ temperature and density increase significantly
→ can balance further mass infall
→ **protostar is dynamically stable**

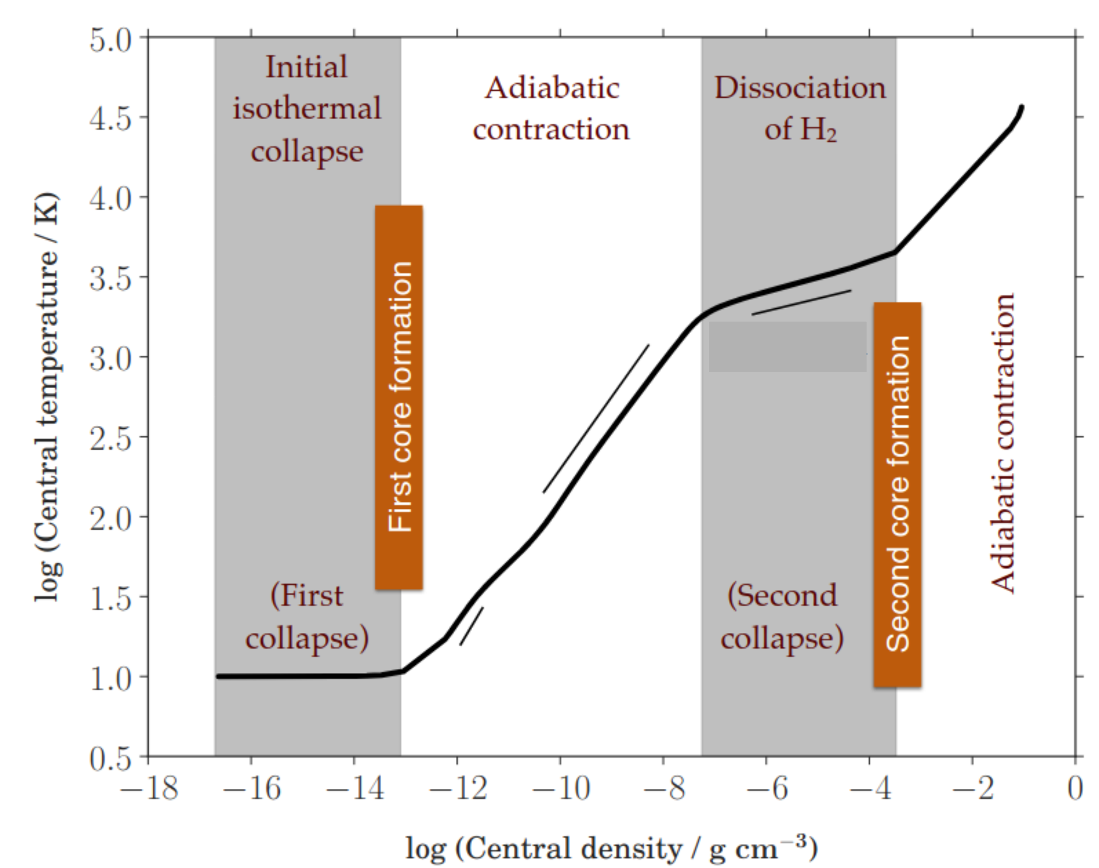

Bhandare et al., A&A 618, A95 (2018)

Accretion luminosity

the protostar is now in its main accretion phase
→ gravitational potential energy due to accretion is radiated into space:
accretion luminosity L_{acc} (→ energy per unit time)

$$L_{\rm acc} \equiv \frac{G\, M_*\, \dot{M}}{R_*}$$
$$= 61\, L_\odot \left(\frac{\dot{M}}{10^{-5}\, M_\odot\, {\rm yr}^{-1}}\right) \left(\frac{M_*}{1\, M_\odot}\right) \left(\frac{R_*}{5\, R_\odot}\right)^{-1}$$

mass accretion rate:

$$\dot{M} = M_*/t$$

(“*” denotes properties of the protostar)

→ this is a good approximation for low-mass protostars
(“Mass-gaining object deriving most of its luminosity from accretion”)

→ high-mass protostars: additional contributions from contraction and early nuclear fusion

Topics today

- The first core and accretion luminosity
- **The protostellar envelope**
- Protostellar evolution
- Pre-main sequence evolution

Section 11.1 in Stahler & Palla

The protostellar envelope

- outer envelope: optically thin
  (observable in far-infrared)

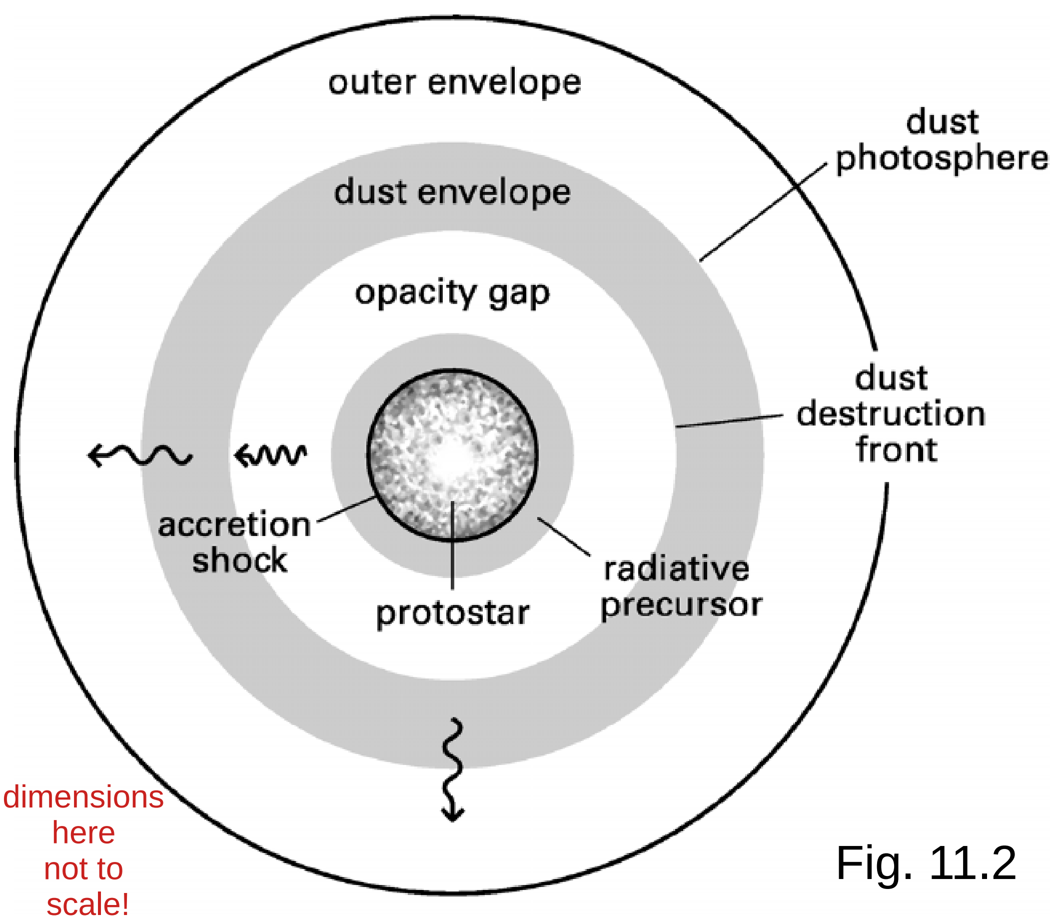

dimensions here not to scale!

Fig. 11.2

The protostellar envelope

- outer envelope: optically thin
  (observable in far-infrared)
- dust photosphere: warm surface
  (observable in the mid-infrared)

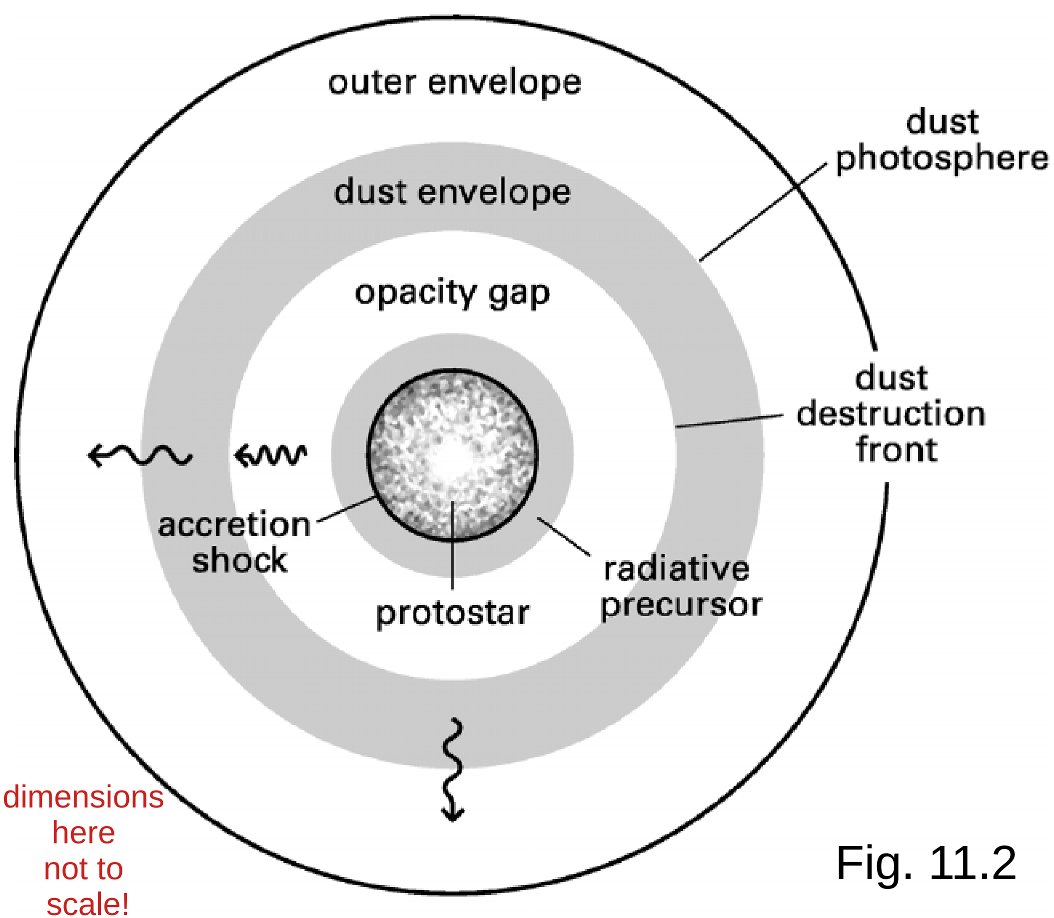

dimensions here not to scale!

Fig. 11.2

The protostellar envelope

- outer envelope: optically thin
  (observable in far-infrared)
- dust photosphere: warm surface
  (observable in the mid-infrared)
- dust envelope: optically thick

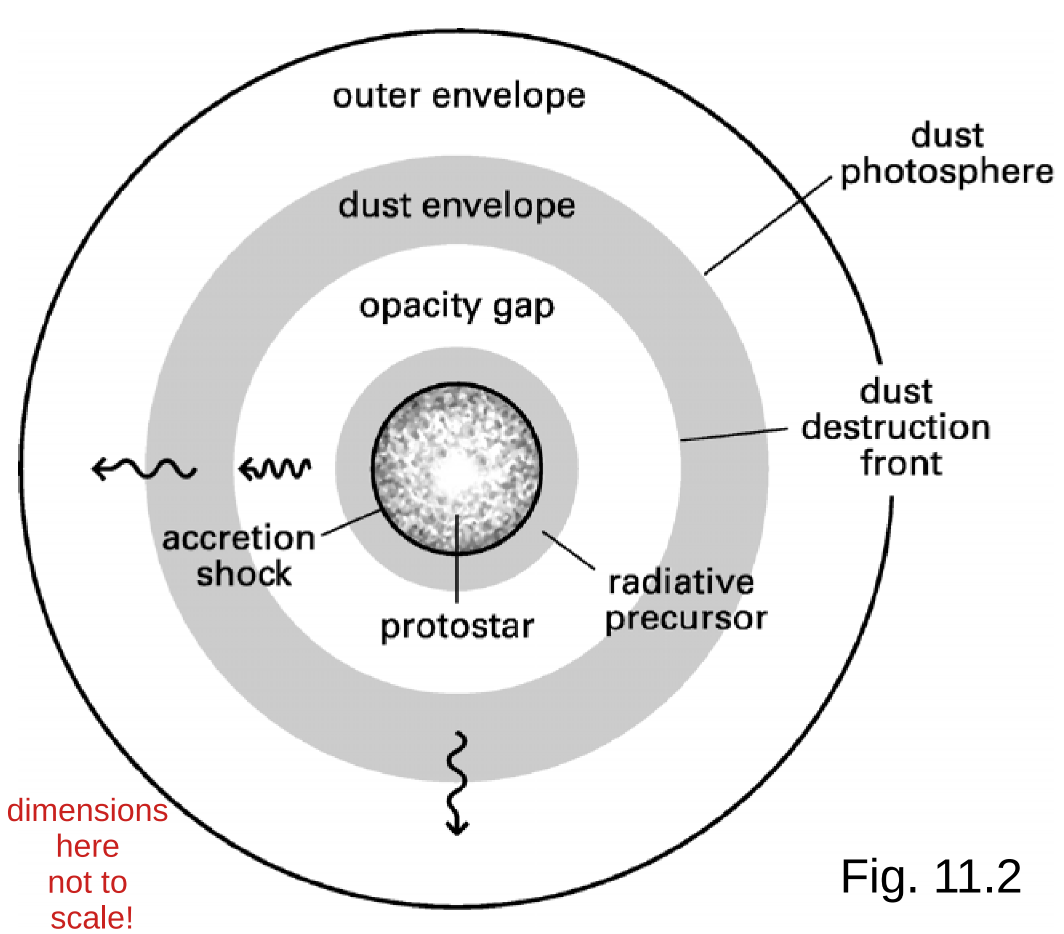

Fig. 11.2

The protostellar envelope

- outer envelope: optically thin
    (observable in far-infrared)
- dust photosphere: warm surface
    (observable in the mid-infrared)
- dust envelope: optically thick
- opacity gap:
    → dust sublimates at T~1500 K
    → reduced opacity
    → infalling gas transparent to protostellar radiation
    → radiation trapped due to high dust opacities
    → dust re-radiates at far infrared

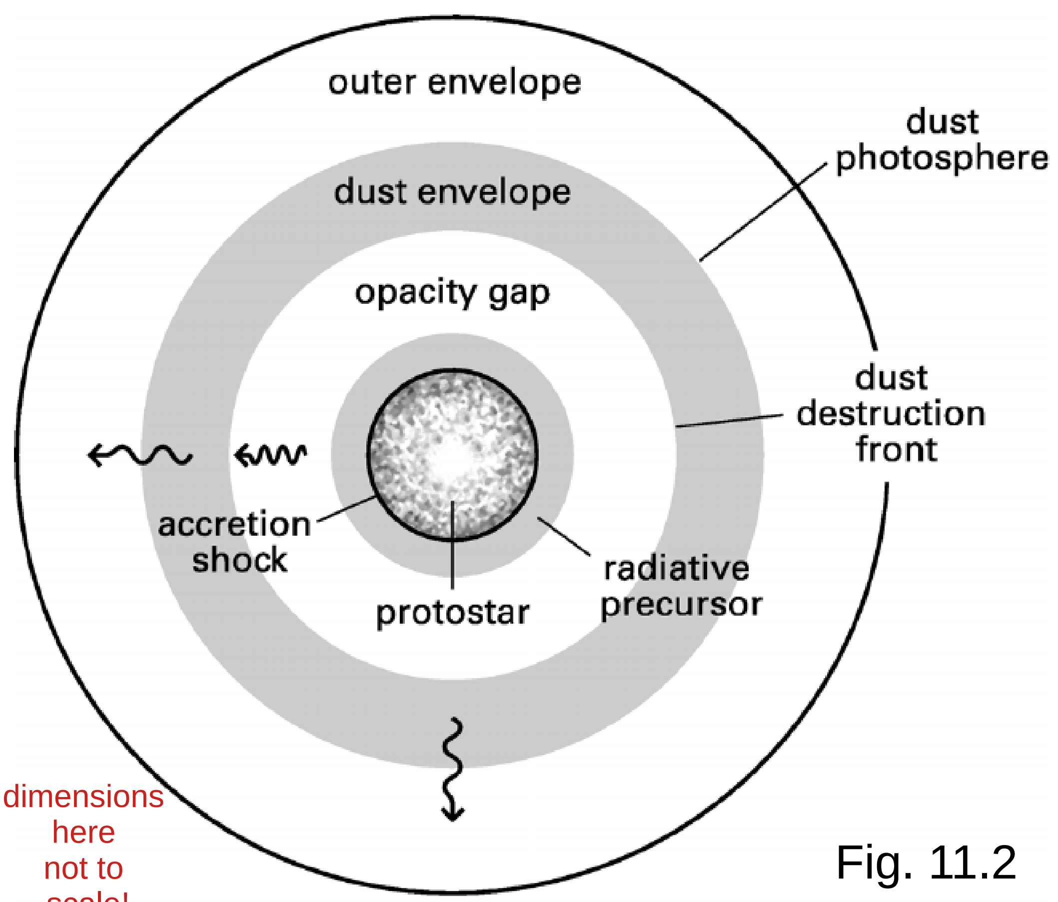

dimensions here not to scale!

Fig. 11.2

The protostellar envelope

- outer envelope: optically thin
  (observable in far-infrared)
- dust photosphere: warm surface
  (observable in the mid-infrared)
- dust envelope: optically thick
- opacity gap:
  → dust sublimates at T~1500 K
  → reduced opacity
  → infalling gas transparent to protostellar radiation
  → radiation trapped due to high dust opacities
  → dust re-radiates at far infrared
- radiative precursor (pre-shock region):
  → gas ionized through collisions
  → opacity rises again

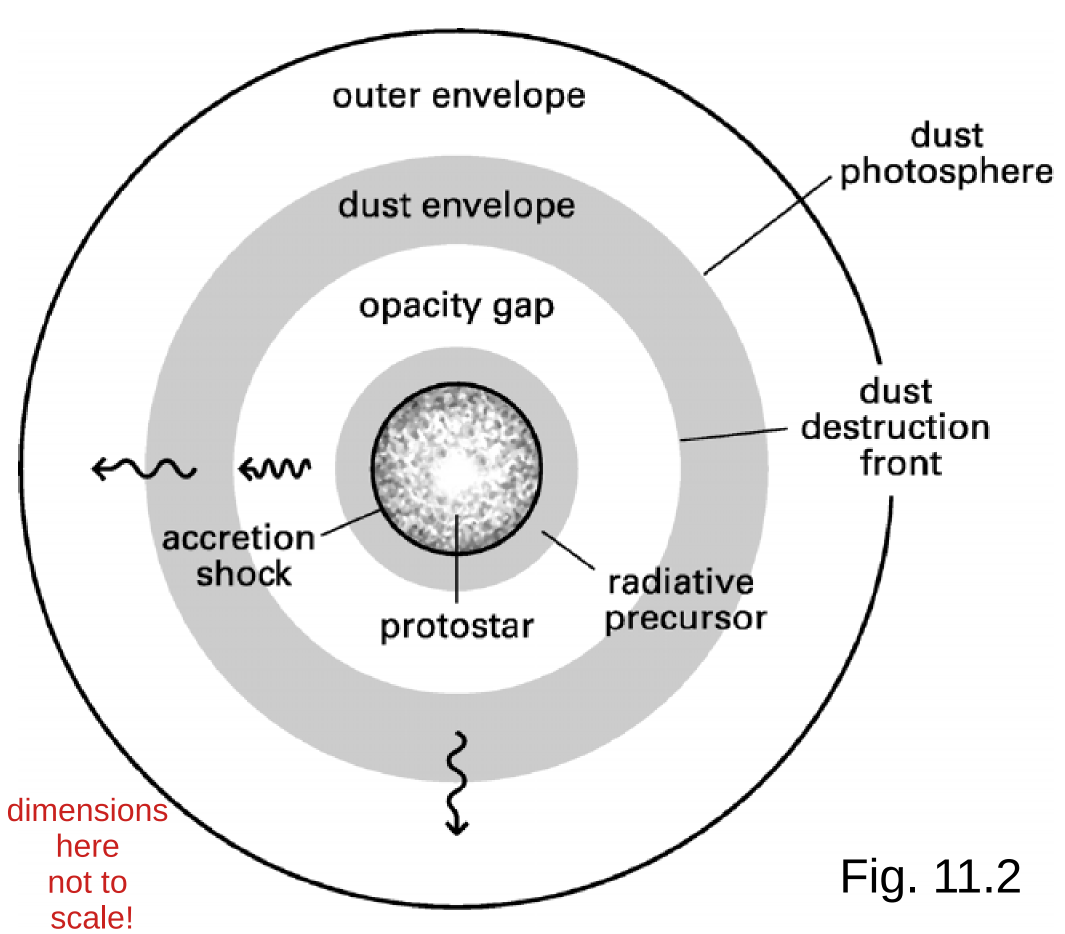

Fig. 11.2

The protostellar envelope

- outer envelope: optically thin
  (observable in far-infrared)
- dust photosphere: warm surface
  (observable in the mid-infrared)
- dust envelope: optically thick
- opacity gap:
  → dust sublimates at T~1500 K
  → reduced opacity
  → infalling gas transparent to protostellar radiation
  → radiation trapped due to high dust opacities
  → dust re-radiates at far infrared
- radiative precursor (pre-shock region):
  → gas ionized through collisions
  → opacity rises again
- accretion shock at the protostar

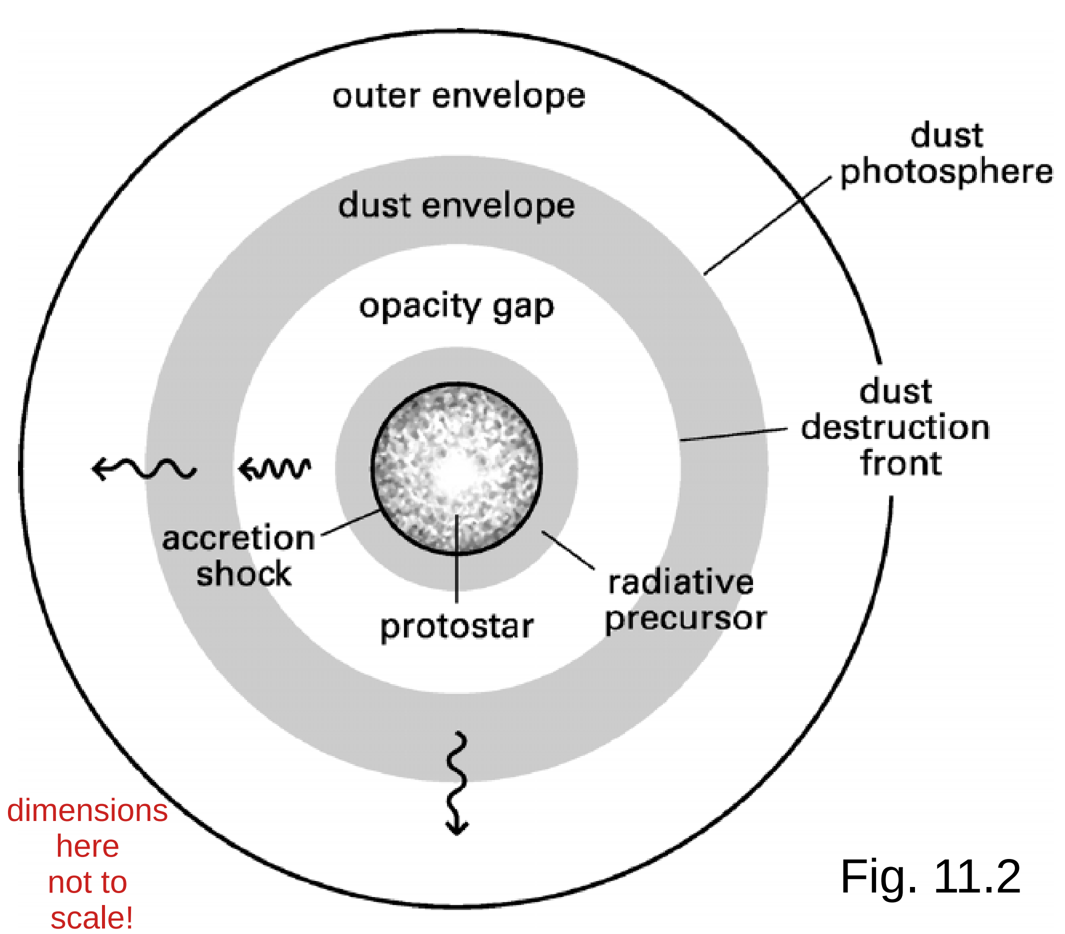

Fig. 11.2

The protostellar envelope

Typical dimensions of a 1M$_\odot$ protostar:

Outer envelope:
a few 100 to a few 1000 or 10^4 AU

Dust photosphere:
~ 10 AU

Dust destruction front: ~ 1 AU

Protostar:
~ 5 R$_\odot$ ~ 0.02 AU

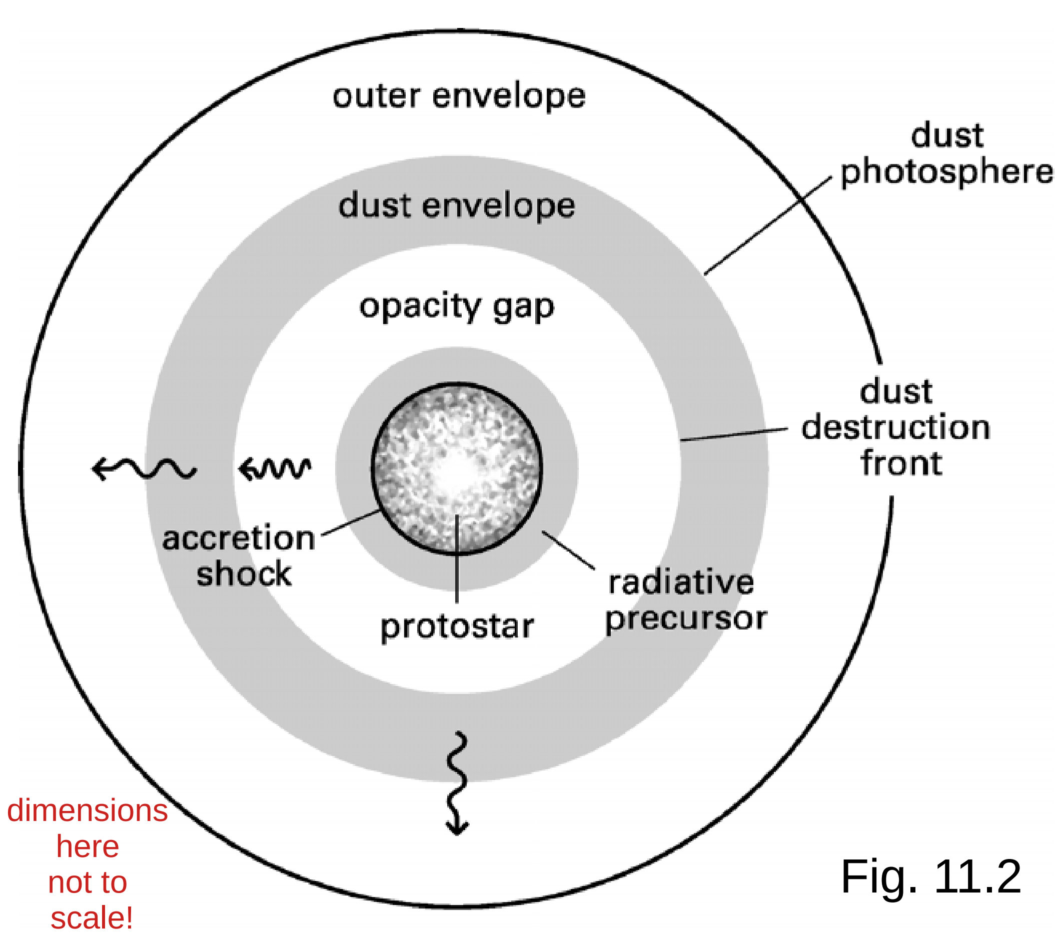

Fig. 11.2

The protostellar envelope

- Difference in radiation
    - from shocked “radiative precursor” (X-ray/optical) and
    - from dust photosphere (mid- to far-infrared)

- At accretion shock location:
    → gas approaches protostar at free-fall speed

$$
\begin{aligned}
V_{\mathrm{ff}} &= \left(\frac{2\,G\,M_*}{R_*}\right)^{1/2} \\
&= 280\ \mathrm{km\ s^{-1}} \left(\frac{M_*}{1\ M_\odot}\right)^{1/2} \left(\frac{R_*}{5\ R_\odot}\right)^{-1/2}
\end{aligned}
$$

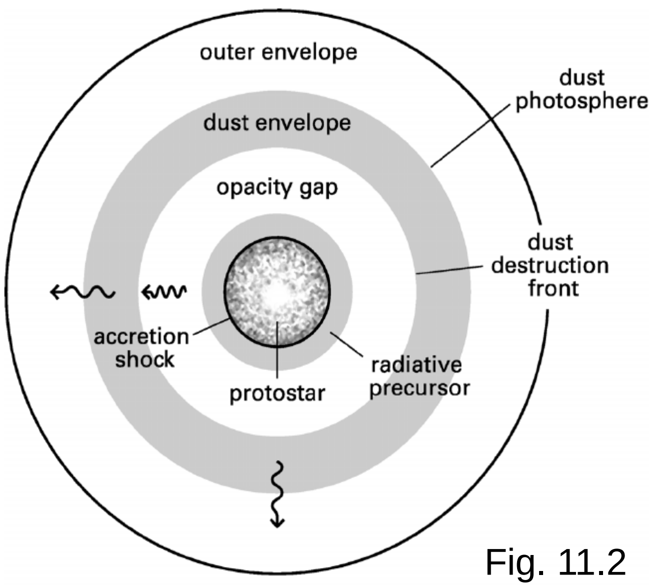

Fig. 11.2

The protostellar envelope

- Immediate postshock temperature >10^6 K (UV and X-ray regime)

- The surface of precursor radiates as a blackbody
→ Stefan Boltzmann law:

$$L_{acc} = 4\pi R_*^2 \sigma_B T_*^4 \qquad L_{acc} \equiv \frac{G M_* \dot{M}}{R_*}$$

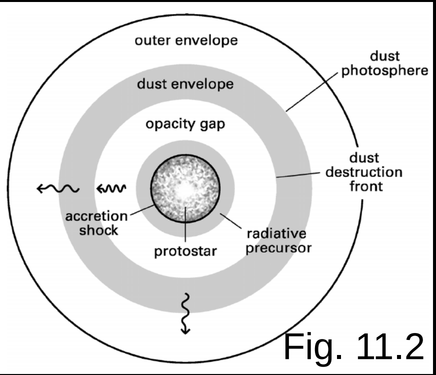

Fig. 11.2

$$T_{eff} \approx \left(\frac{G M_* \dot{M}}{4\pi \sigma_B R_*^3} \right)^{1/4}$$

$$= 7300\ \mathrm{K} \left(\frac{\dot{M}}{10^{-5}\ M_\odot\ \mathrm{yr}^{-1}} \right)^{1/4} \left(\frac{M_*}{1\ M_\odot} \right)^{1/4} \left(\frac{R_*}{5\ R_\odot} \right)^{-3/4}$$

→ Opacity gap is bathed in “optical emission” similar to a main-sequence star (very different to observable dust photosphere!)

Temperature of the envelope

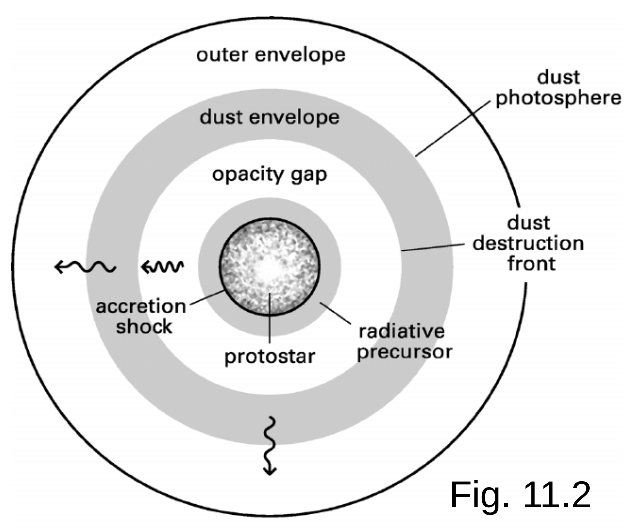

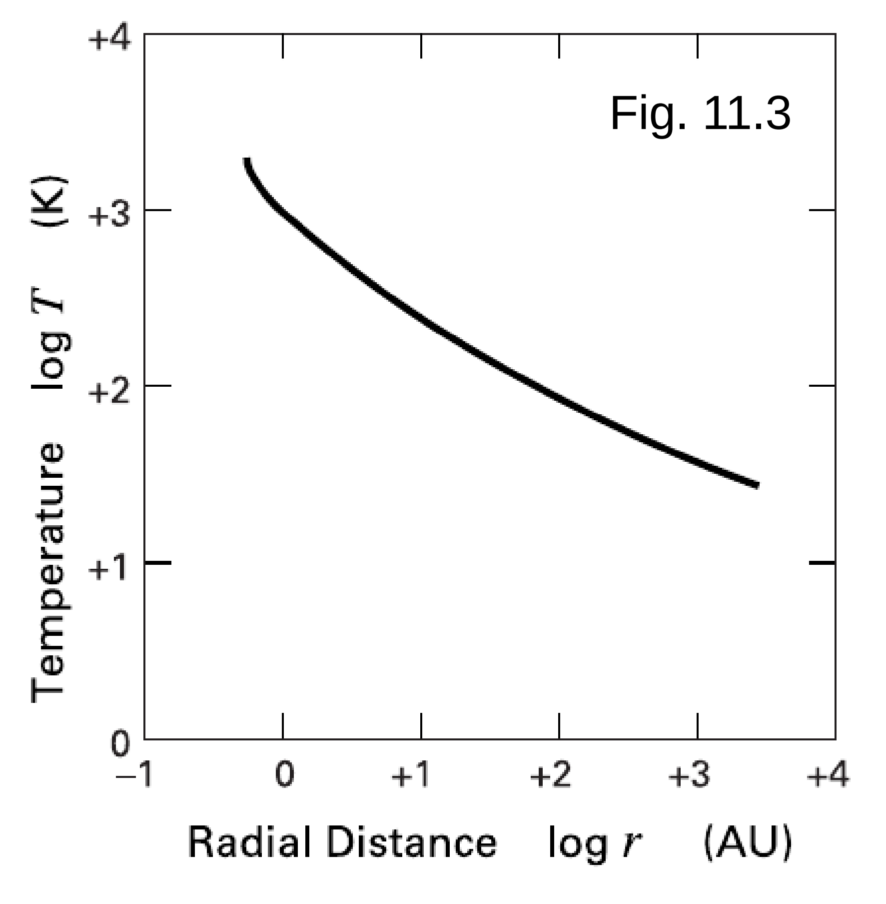

power-law profiles:

optically thick dust envelope: $T(r) \sim r^{-0.8}$

optically thin outer envelope: $T(r) \sim r^{-0.4}$

simulation of the formation of a protostar:

https://www.youtube.com/watch?v=lhkjP74RayI

Bhandare et al., A&A 618, A95 (2018)

Topics today

- The first core and accretion luminosity
- The protostellar envelope structure
- **Protostellar evolution**
- Pre-main sequence evolution

Sect. 11.2 and 11.4 in Stahler & Palla

Stellar structure equations

M_r: mass within shells of radius **r**

$$\frac{\partial r}{\partial M_r} = \frac{1}{4\,\pi\,r^2\,\rho}$$

$$M_r \equiv \int_0^r 4\,\pi\,r^2 \rho\,dr$$

ρ: density

→ each new shell represents matter that has just passed through the shock front and settled onto the hydrostatic surface

stellar structure equations help us to understand
what physical processes are happening within the interior of the protostar itself

Stellar structure equations

M_r: mass within shells of radius r

$$\frac{\partial r}{\partial M_r} = \frac{1}{4\,\pi\,r^2\,\rho}$$

hydrostatic equilibrium

$$\frac{\partial P}{\partial M_r} = -\frac{G\,M_r}{4\,\pi\,r^4}$$

ideal gas:

$$P = \frac{\rho}{\mu}\mathcal{R}\,T$$

μ(ρ,T): mean molecular weight

Stellar structure equations

M_r: mass within shells of radius r

$$\frac{\partial r}{\partial M_r} = \frac{1}{4\,\pi\,r^2\,\rho}$$

hydrostatic equilibrium

$$\frac{\partial P}{\partial M_r} = -\frac{G\,M_r}{4\,\pi\,r^4}$$

thermal structure: diffusion equation

$$T^3\,\frac{\partial T}{\partial M_r} = -\frac{3\,\kappa\,L_{\rm int}}{256\,\pi^2\,\sigma_B\,r^4}$$

σ_B: Boltzmann constant
L_{int}: interior luminosity
$\kappa(\rho,T)$: mean opacity

Stellar structure equations

M_r: mass within shells of radius r

$$\frac{\partial r}{\partial M_r} = \frac{1}{4\,\pi\,r^2\,\rho}$$

hydrostatic equilibrium

$$\frac{\partial P}{\partial M_r} = -\frac{G\,M_r}{4\,\pi\,r^4}$$

s(ρ,T): specific entropy
→ heat content of the associated mass shell

thermal structure: diffusion equation

$$T^3\,\frac{\partial T}{\partial M_r} = -\frac{3\,\kappa\,L_{\mathrm{int}}}{256\,\pi^2\,\sigma_B\,r^4}$$

internal luminosity: heat equation

$$\frac{\partial L_{\mathrm{int}}}{\partial M_r} = \epsilon - T\,\frac{\partial s}{\partial t}$$

ε(ρ,T): nuclear energy release rate

Stellar structure equations

M_r: mass within shells of radius r

$$\frac{\partial r}{\partial M_r} = \frac{1}{4\,\pi\,r^2\,\rho}$$

hydrostatic equilibrium

$$\frac{\partial P}{\partial M_r} = -\frac{G\,M_r}{4\,\pi\,r^4}$$

thermal structure: diffusion equation

$$T^3\,\frac{\partial T}{\partial M_r} = -\frac{3\,\kappa\,L_{\rm int}}{256\,\pi^2\,\sigma_B\,r^4}$$

internal luminosity: heat equation

$$\frac{\partial L_{\rm int}}{\partial M_r} = \epsilon - T\,\frac{\partial s}{\partial t}$$

→ **with appropriate boundary conditions: follow protostellar evolution numerically**

Mass-radius relation of a Sun-like star

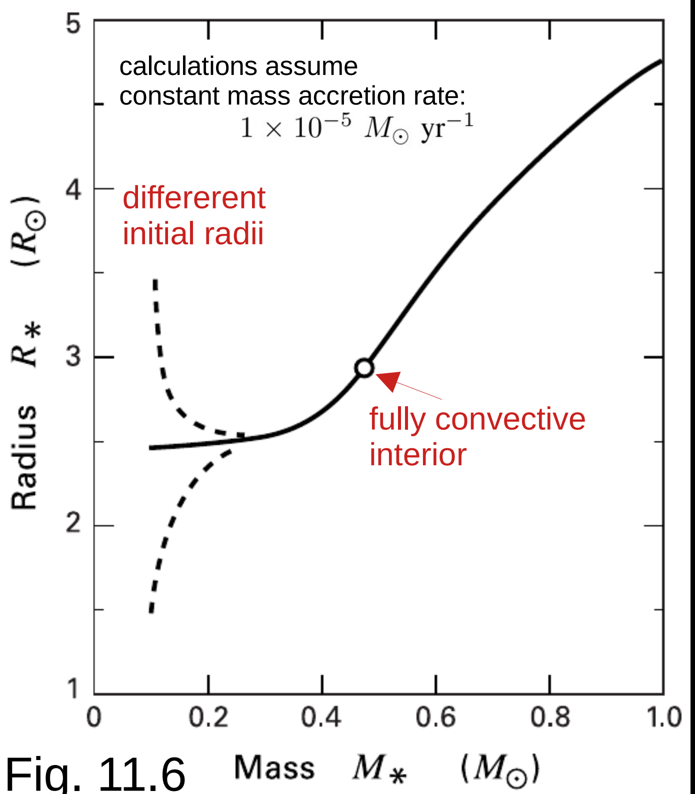

Fig. 11.6

- protostar can be described by **entropy profile $s(M_r)$**
  → changing conditions at the accretion shock front
- in absence of nuclear burning, but mass infall:
  → increasing **$s(M_r)$ profile** → **increasing R_***
- assume different initial radii:
- large initial radius:
  → low v_{ff}
  → weak shock
  → entropy lowers
  → radius shrinks
- opposite effect for small initial radius

$$V_{\mathrm{ff}} = \left(\frac{2\,G\,M_*}{R_*}\right)^{1/2}$$

- s represents heat content of each added mass shell
→ increase of $s(M_r)$ causes a swelling of the protostar

Convection

surface

center

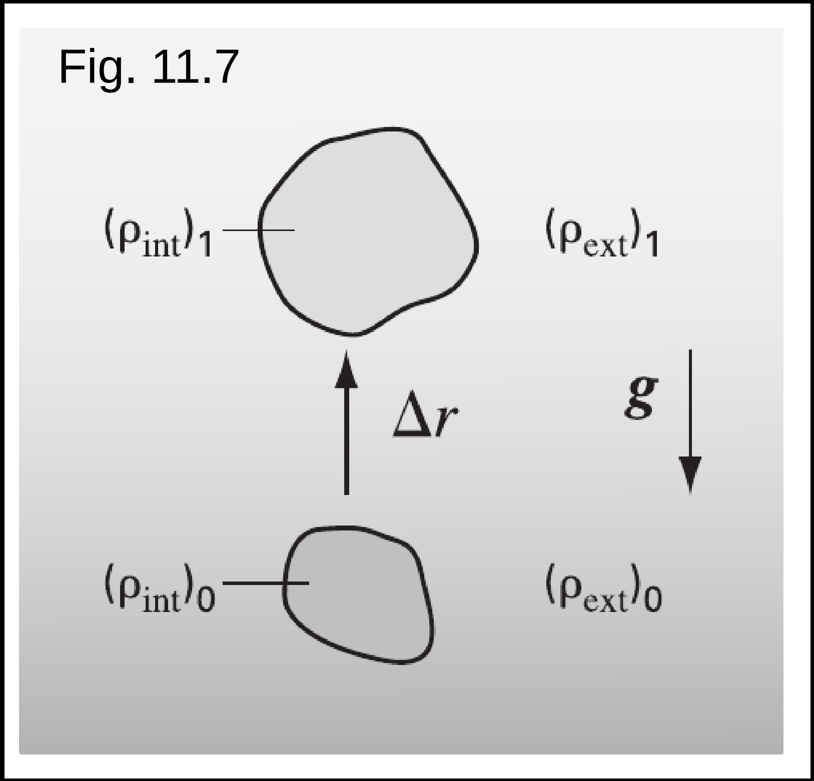

- displace parcel by Δr towards protostellar surface

- to maintain pressure balance:
  → expansion
  → density decreases

<u>two possible scenarios:</u>

- large density change:
  → **convectively unstable**
  → parcel moves towards surface
  → important heat transport mechanism

$$(\rho_{\rm int})_1 > (\rho_{\rm ext})_1$$

- small density change:
  → **radiatively stable**
  → parcel sinks back down

Convection

surface

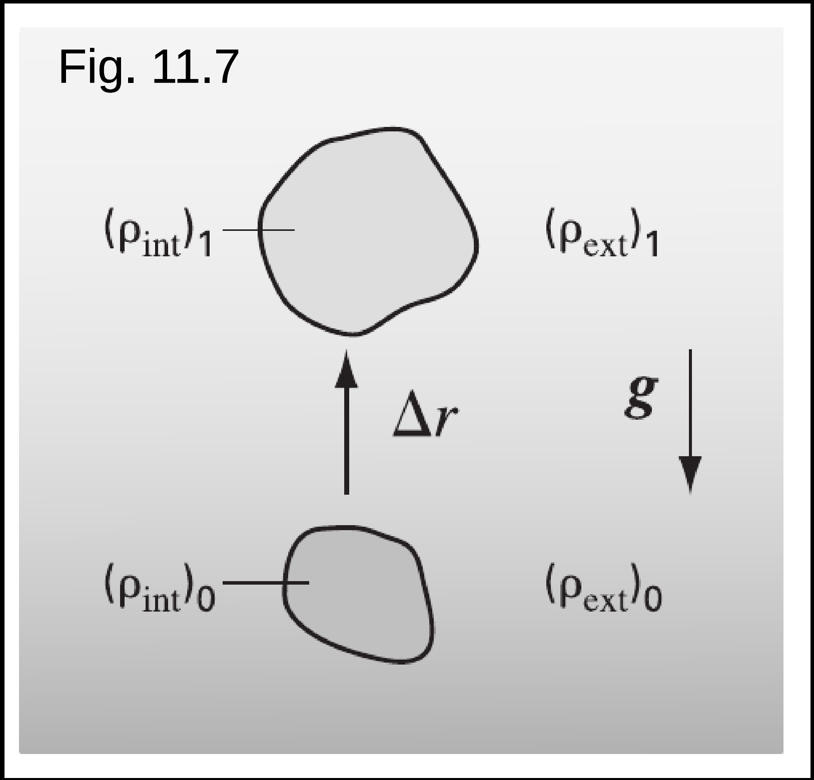

center

- Schwarzschild's criterion: $\partial s/\partial M_r > 0$

→ **a rising entropy profile implies radiative stability**

→ **accretion shock at the protostar surface leads to a structure in which heat is transported outward by radiation, rather than convective motion**

Convection

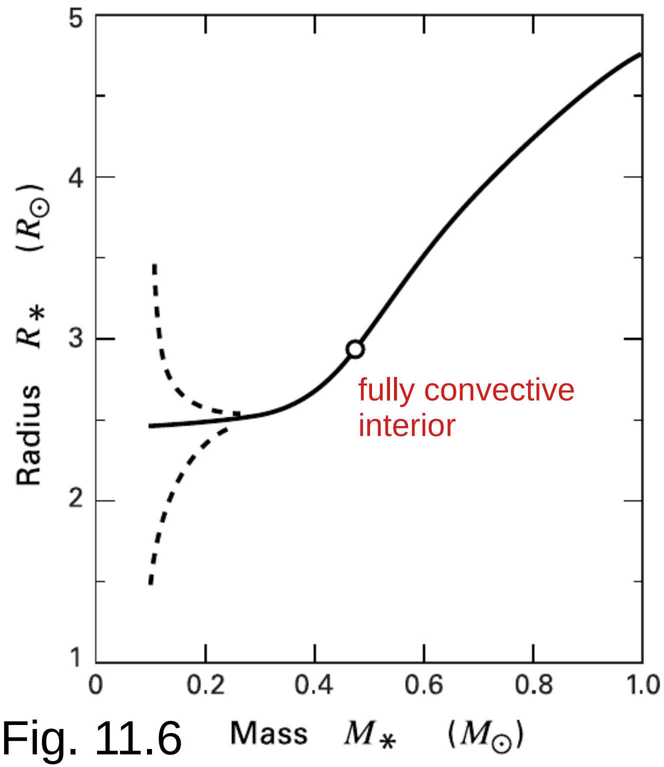

Fig. 11.6

- M_*/R_* rises fast
  - → T in center increases
  - → **ignition of nuclear fusion (D-burning)**
- increase of central entropy $\partial s/\partial M_r < 0$
  - → **protostar becomes convectively unstable**

Deuterium burning

^{2}H = D

$$^2\mathrm{H} + {}^1\mathrm{H} \rightarrow {}^3\mathrm{He} + \gamma \qquad \Delta E_D \equiv 5.5\,\mathrm{MeV}$$

- exothermic reaction
- reaction rate highly sensitive to temperature

→ **deuterium burning starts at T ~10^6 K**

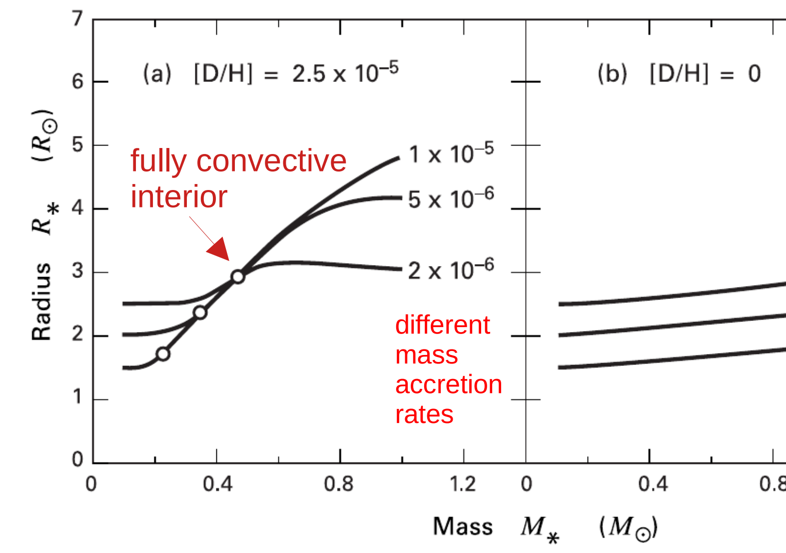

Fig. 11.8

- increase of T → more deuterium burning → more heat
- increase of protostellar radius → lower T in the center again
- **deuterium burning acts as kind of thermostat keeping protostellar core at that evolutionary stage at about 10^6 K**

→ steady supply by new deuterium from infalling gas via convection necessary to maintain thermostat

Radiative stability

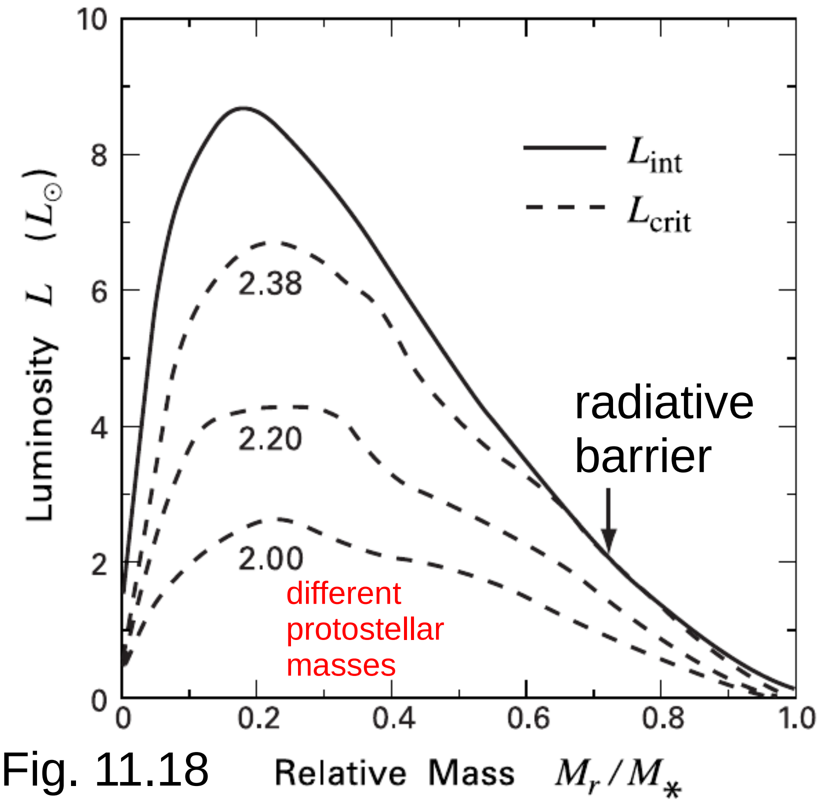

Fig. 11.18

- **if M > 1M$_\odot$ return to radiative stability:**
  decline in the average opacity,
  easier for the interior luminosity to reach surface

- Kramers law: κ is proportional to $\rho T^{-7/2}$

- **Critical luminosity L_{crit}:**
  maximum value of L_{int} carried by radiative diffusion
  (depends on opacity of gas/plasma)

- stellar structure equations:
  L_{crit} is proportional to $M_*^{11/2} R_*^{-1/2}$

- **growing protostars**
  → **L_{crit} rises sharply surpassing L_{int}**
  → **convection then disappears**
  → **protostar gets radiative barrier**

Deuterium shell burning

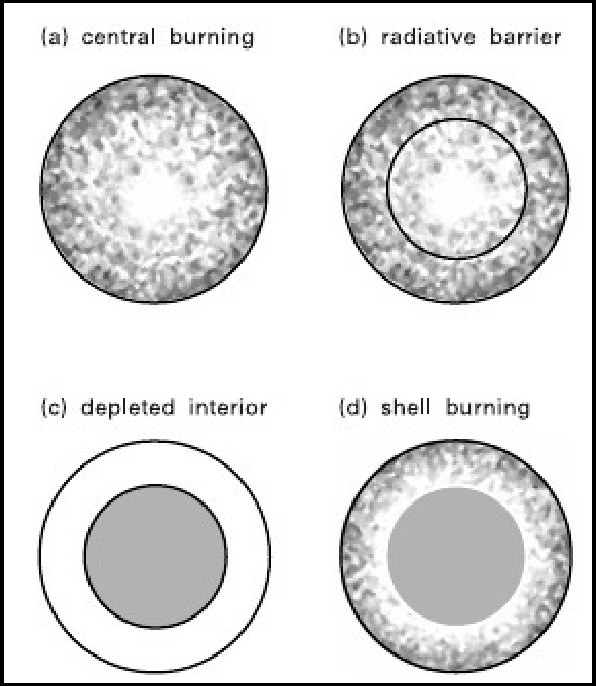

Fig. 11.20

- if $M > 1M_\odot$:

- radiative barrier:
  → no new deuterium to center, remaining D consumed rapidly
- interior luminosity L_{int} declines below L_{crit}
  → convection disappears in whole interior volume
- deuterium accumulates in mantle outside radiative barrier
- no internal fuel
  → R_* does not change much anymore
  → M_*/R_* rises more quickly, and temperatures increase rapidly

- Base of deuterium shell reaches 10^6K,
→ deuterium shell burning starts and
→ convection occurs in this shell structure

Deuterium shell burning

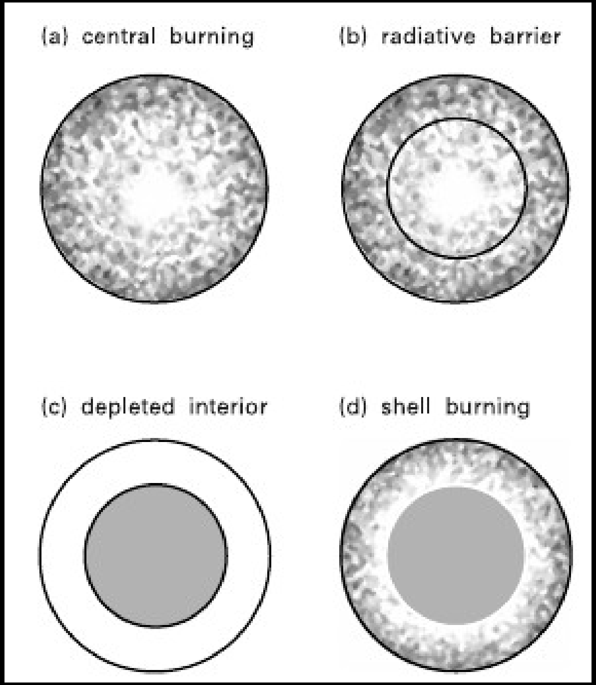

Fig. 11.20

- if M > 1M$_\odot$:

- deuterium shell burning accompanied by structural change of protostar
- shell burning injects heat
  → rises entropy s of the outer layers
  → further swelling of the protostar
- Adding more mass
  → rise of Lcrit
  → drives the radiative barrier & burning layer & convection zone outward

→ **Protostar (>~2M$_\odot$) then almost fully radiatively stable**

Mass-radius relation

of more massive stars!

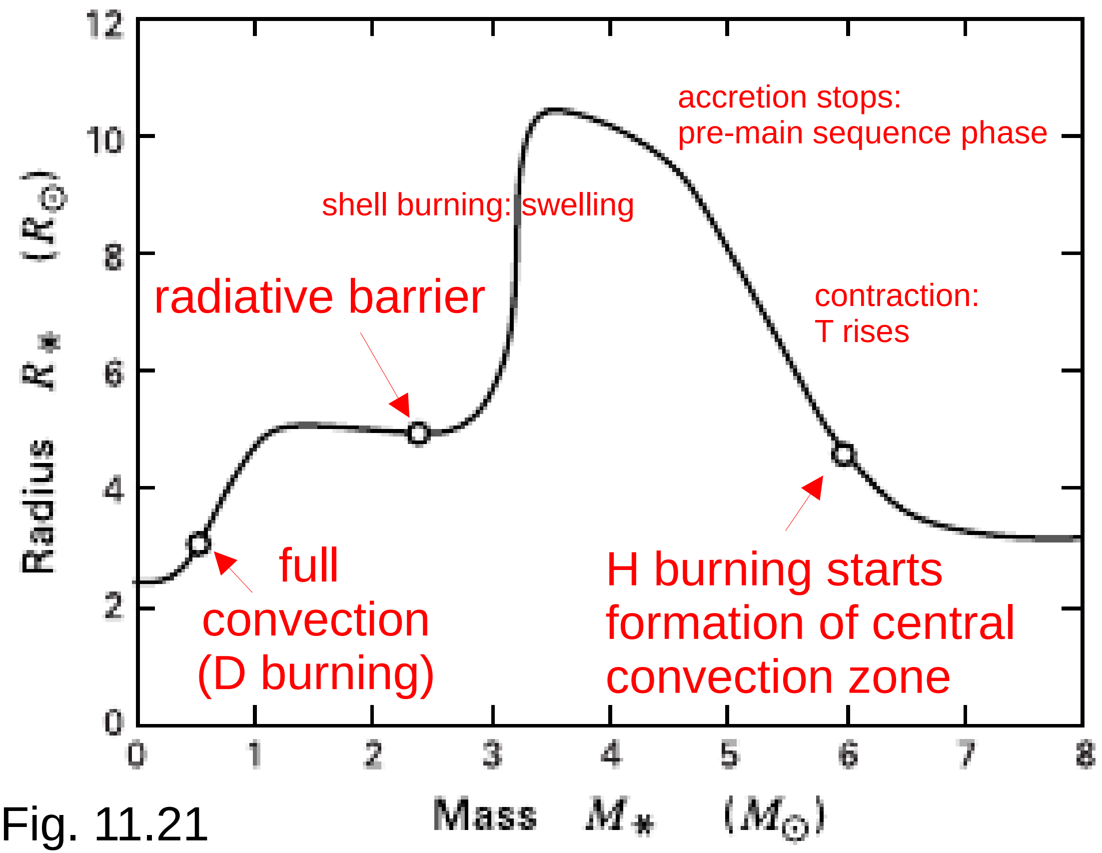

Fig. 11.21

Topics today

- The first core and accretion luminosity
- The protostellar envelope structure
- Protostellar evolution
- **Pre-main sequence evolution**

Chapter 16 in Stahler & Palla

Pre-main-sequence evolution

Protostellar vs. pre-main sequence (PMS) evolution
(mainly for low-mass protostars):

- **Accretion stops**
  → protostar contracts
  → **main luminosity not due to accretion but due to gravitational contraction**

Pre-main-sequence evolution

Different evolution for low- and high-mass PMS stars!

- Low-mass:
    - still convective & deuterium burning
    - **radius shrinks**
      (→ Hayashi tracks)
    - L_{int} falls below Lcrit
      → radiative core forms again
        with shrinking outer convective layer
    - **during further slow contraction internal energy, temperature & luminosity rise again until hydrogen burning starts → zero age main sequence (ZAMS)**
    - Stars below ~$0.4 M_\odot$ reach the ZAMS still fully convective

Pre-main-sequence evolution

Different evolution for low- and high-mass PMS stars!

- Intermediate- to high-mass:

  - More massive stars not convective anymore but fully radiative
    - → no phase of decreasing luminosity
    - → Always gain luminosity and temperature via gravitational energy (and decreasing deuterium shell burning)

  - Hydrogen ignites
    - → ZAMS

Hertzsprung-Russell diagram

Recap:
Hertzsprung-Russell diagram (HRD)
for stars and
more evolved objects

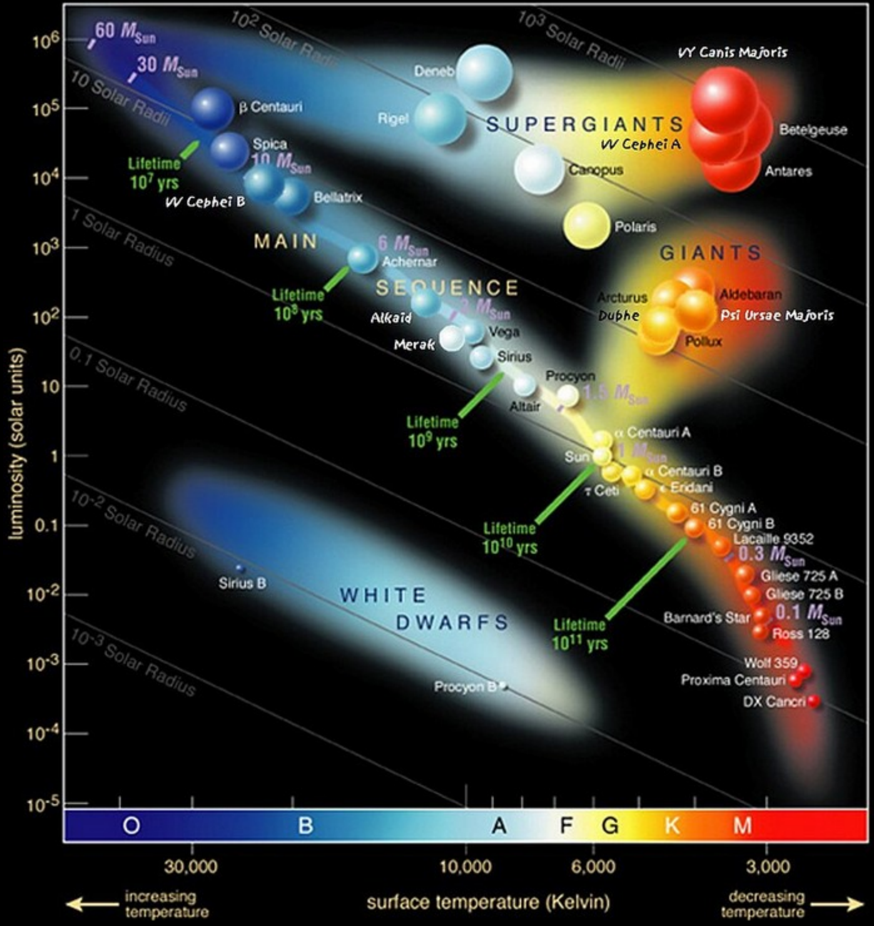

Hertzsprung-Russel diagram

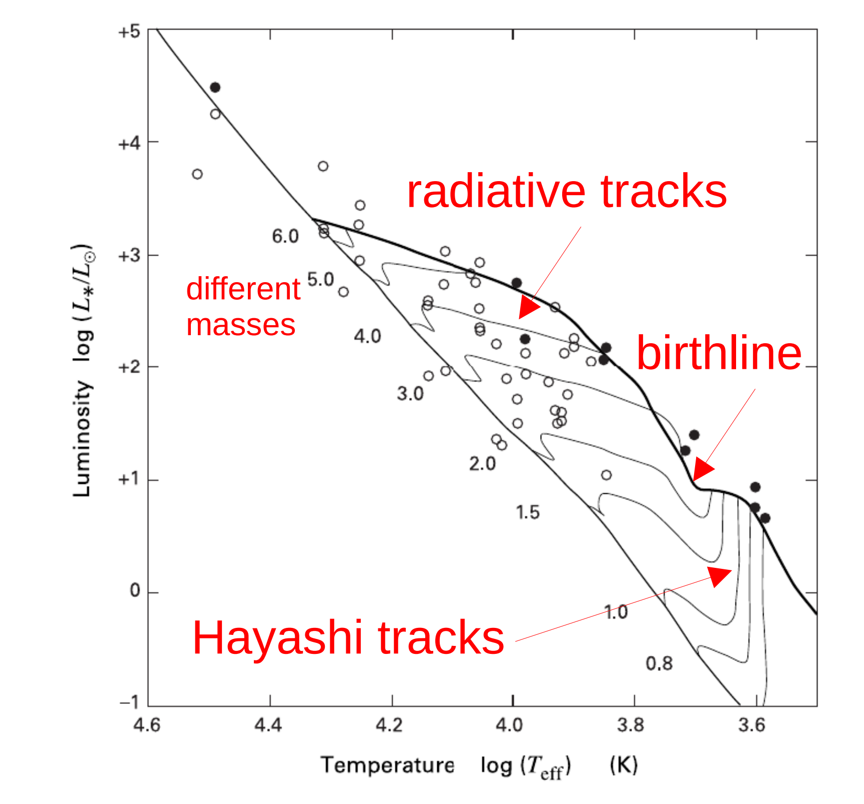

- birthline observationally:

  → locus where stars first appear in the HRD emanating from their dusty natal envelope

- theoretically: birthline the time where main accretion has stopped

- low-mass stars:

  → PMS star gains its luminosity from grav. contraction

  → vertical Hayashi tracks

Hertzsprung-Russel diagram

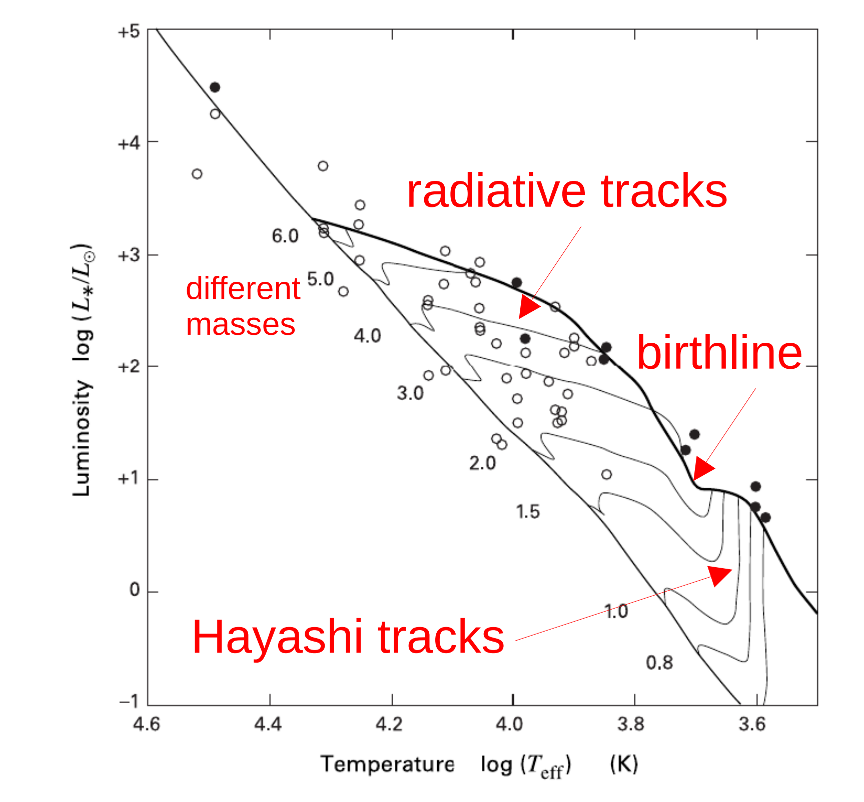

- **Intermediate-mass protostars:**
  fully radiative when stopping accretion
  → no vertical Hayashi part
  but direct horizontal radiative tracks

- **High-mass stars:**
  → start nuclear H-burning and
  entering the ZAMS before accretion ends

  → no (visible) PMS evolution since H-burning
  starts still deeply embedded in their natal cores

Observable spectral energy distributions

Recap:
spectral energy distribution (SED) of a black body

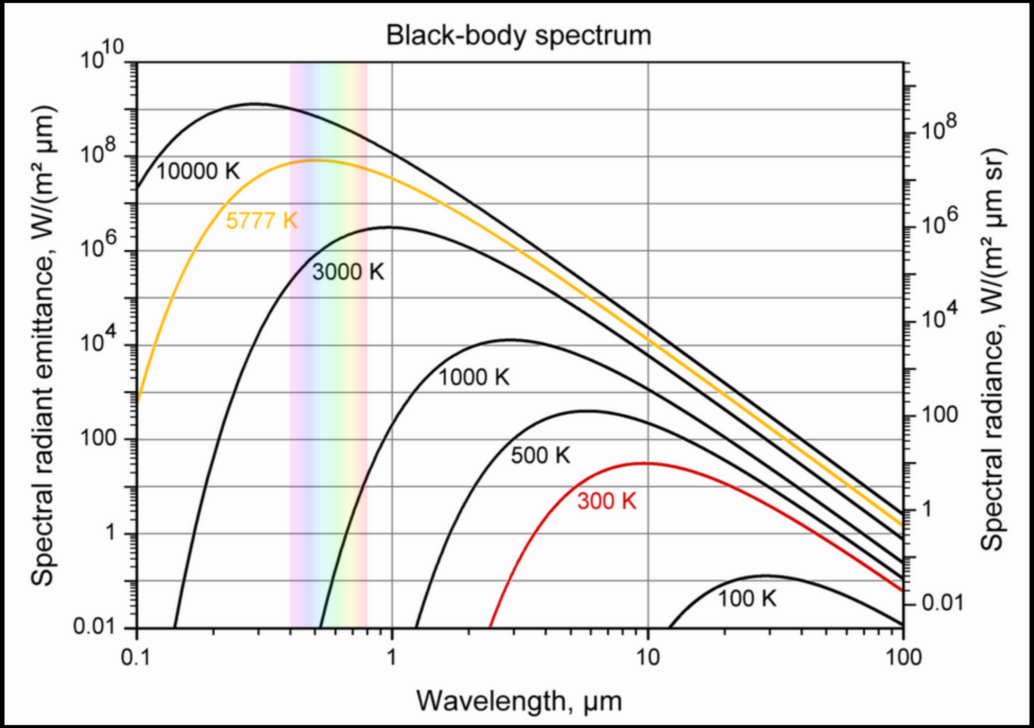

Observable spectral energy distributions

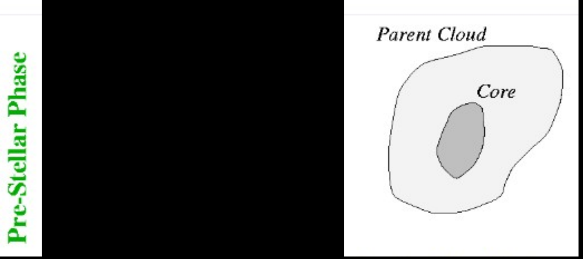

Credit: Philippe André

Observable spectral energy distributions

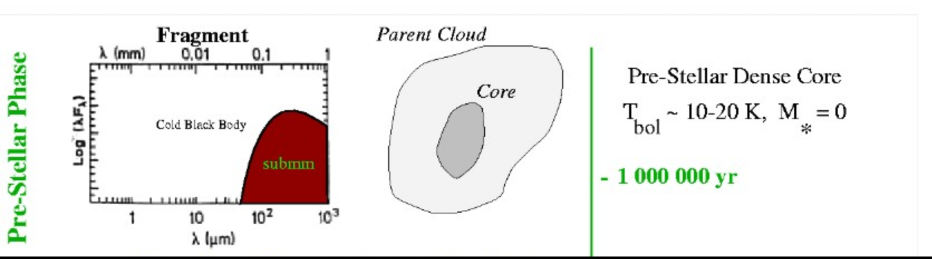

Credit: Philippe André

Observable spectral energy distributions

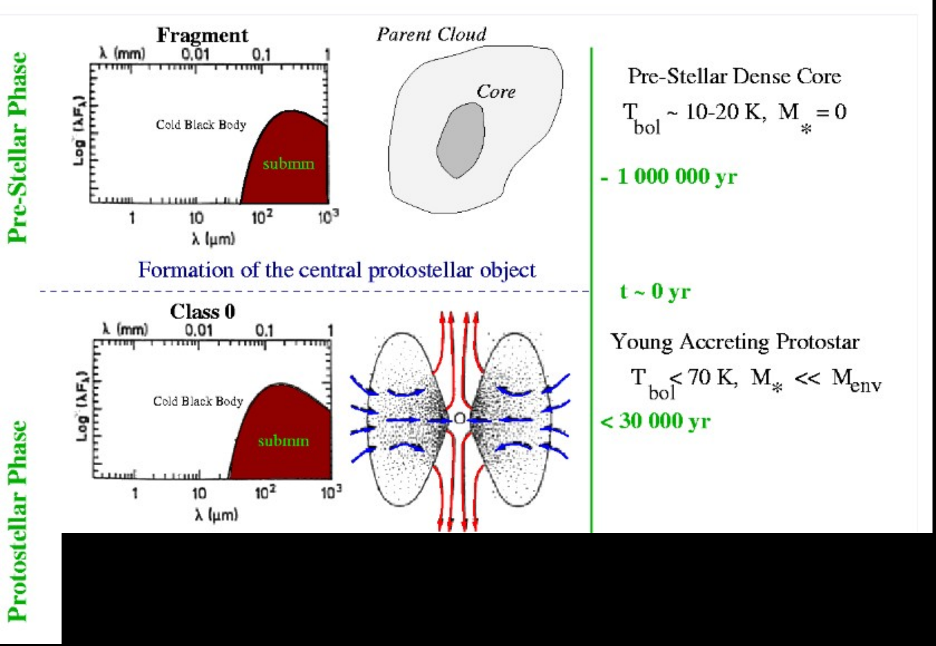

Credit: Philippe André

Observable spectral energy distributions

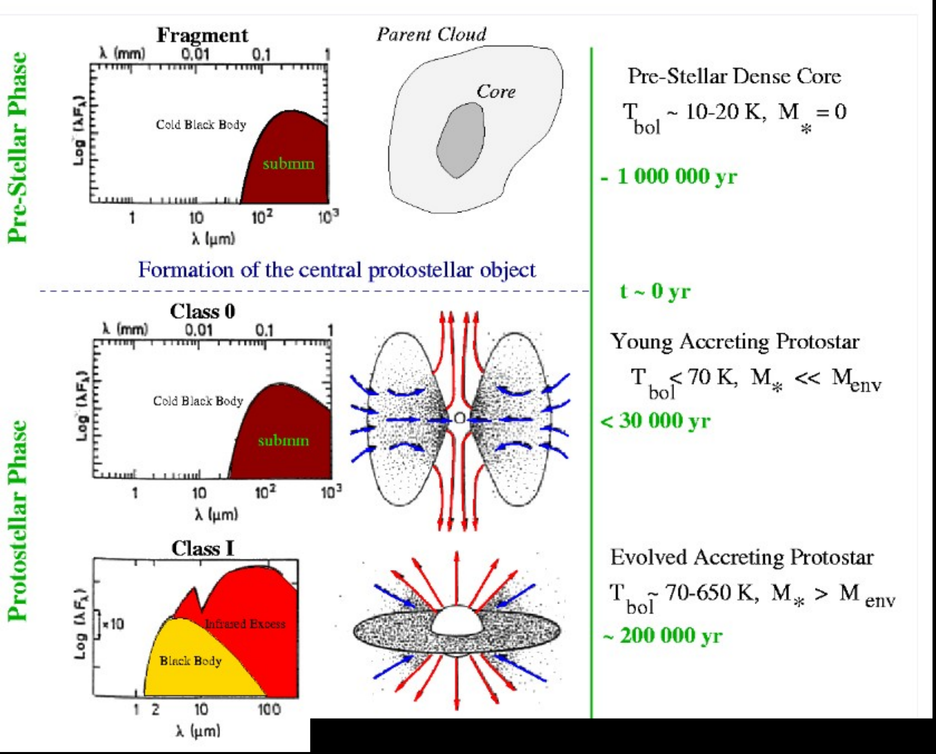

Credit: Philippe André

Observable spectral energy distributions

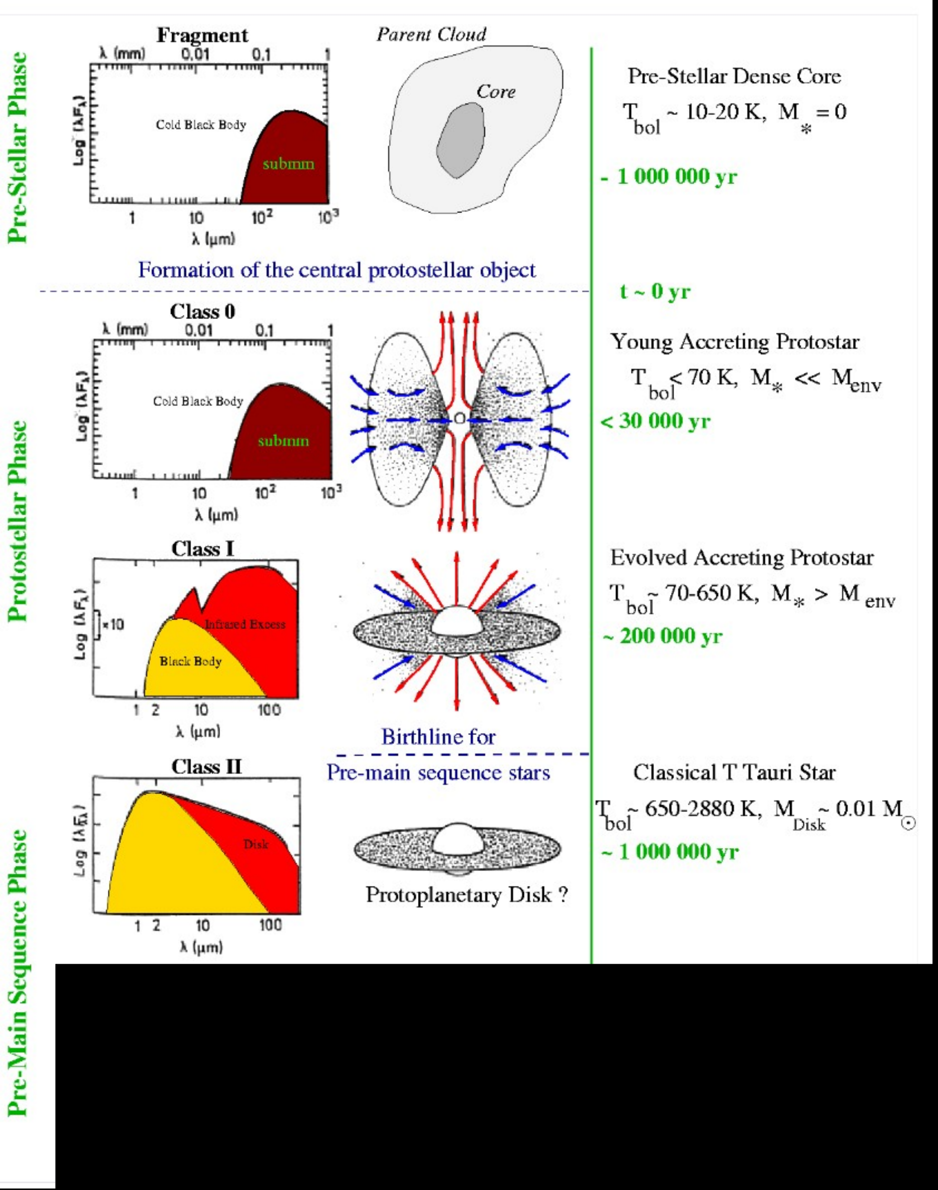

Credit: Philippe André

Observable spectral energy distributions

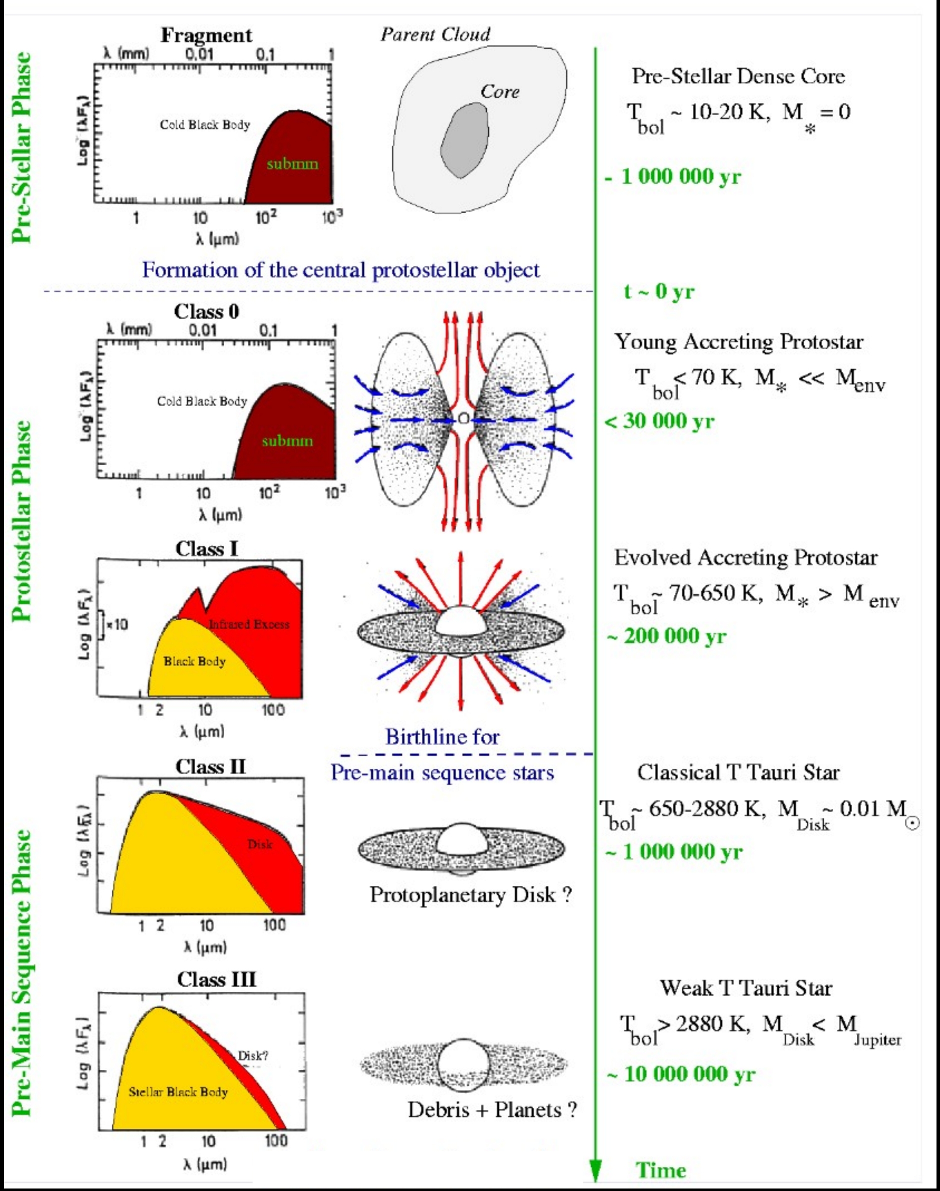

Credit: Philippe André

Observable spectral energy distributions

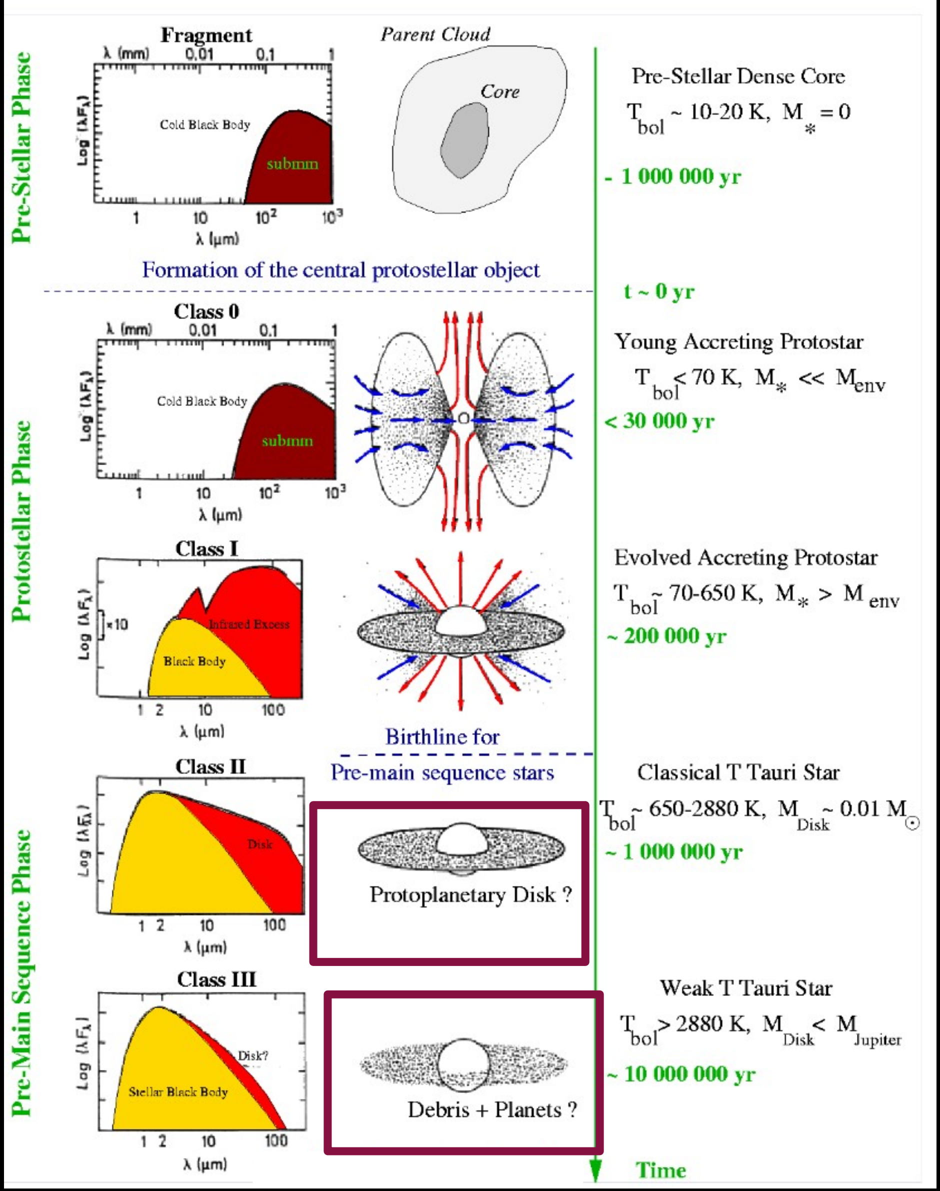

Credit: Philippe André

class I-II disk: HL Tau

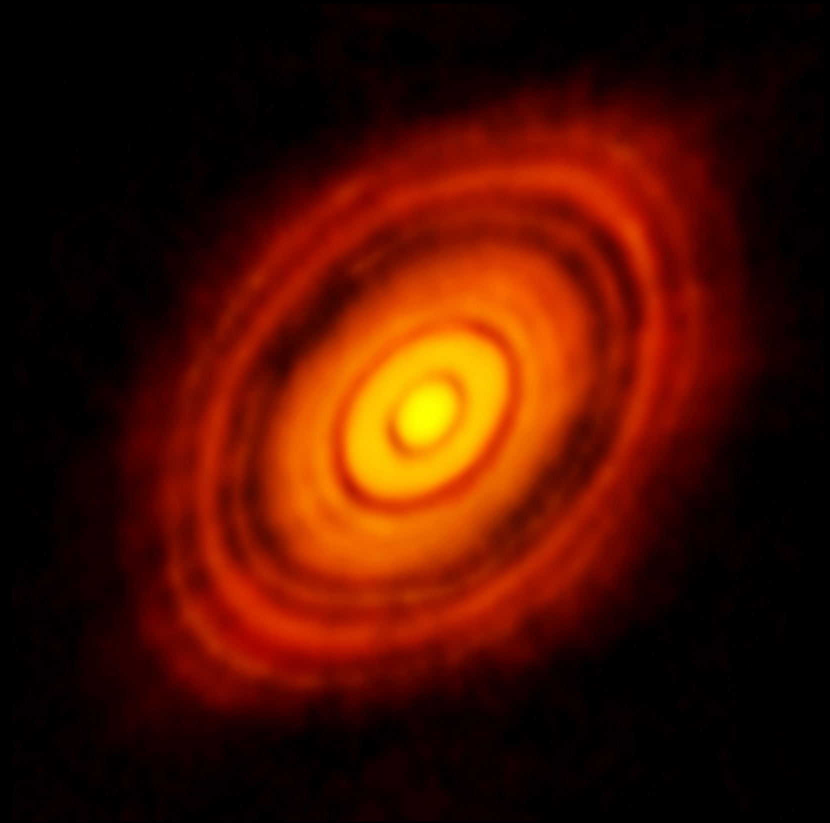

Credit: ALMA (ESO/NAOJ/NRAO)

debris disk: Fomalhaut

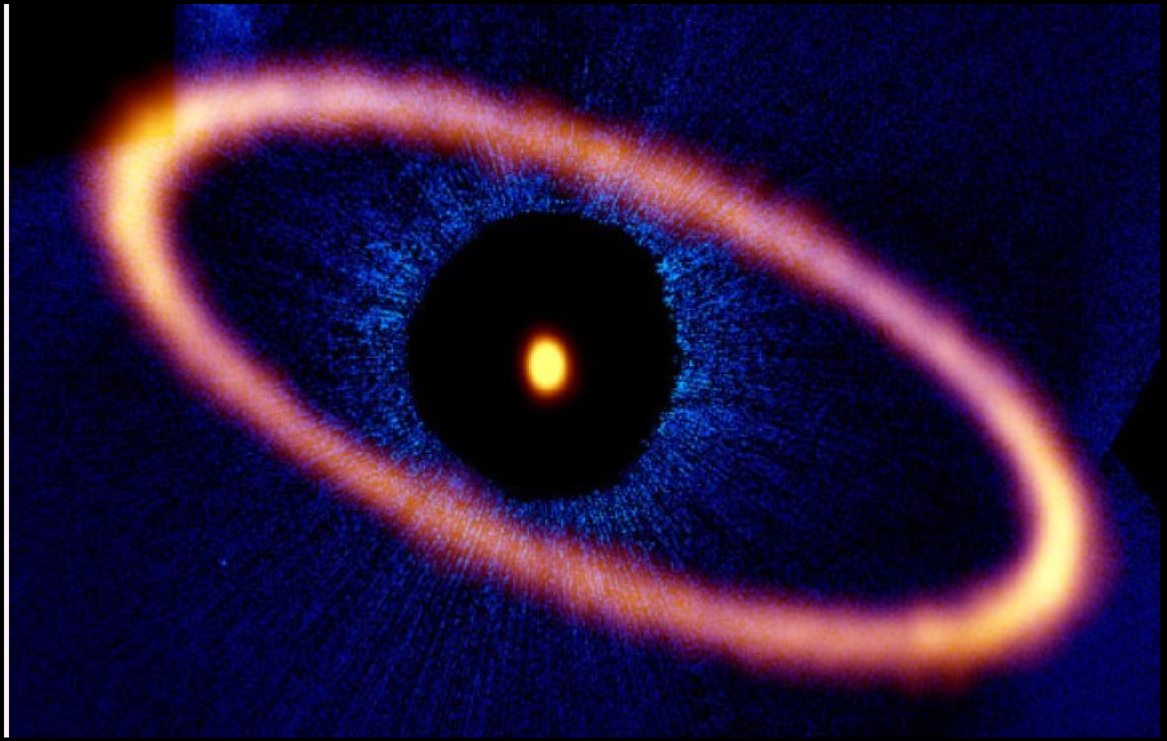

Image credit: ALMA / ESO / NAOJ / NRAO / M. MacGregor / NASA / ESA / Hubble / P. Kalas / B. Saxton / AUI / NSF.

Disk Substructures at High Angular Resolution Project (DSHARP)

Class II disks

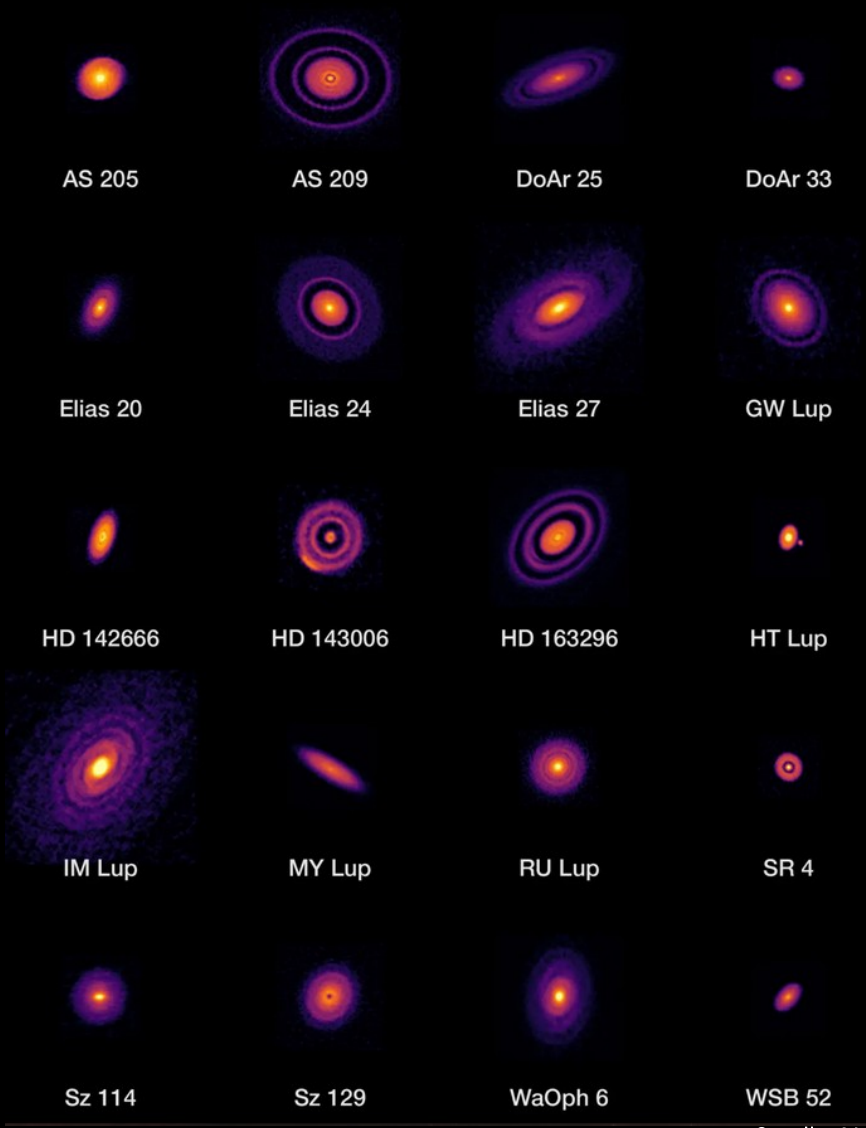

Credit: ALMA (ESO/NAOJ/NRAO), S. Andrews et al.; N. Lira

PDS 70: protoplanets!

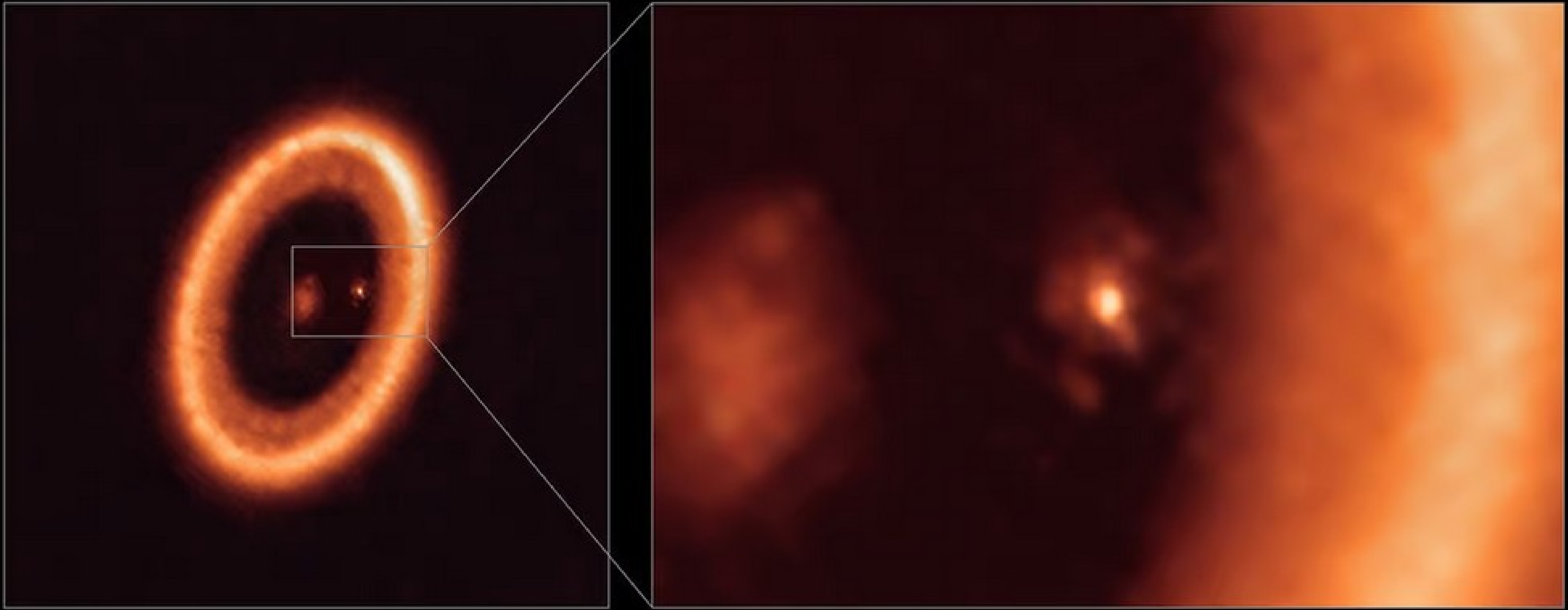

ALMA (ESO/NAOJ/NRAO)/Benisty et al.

Summary

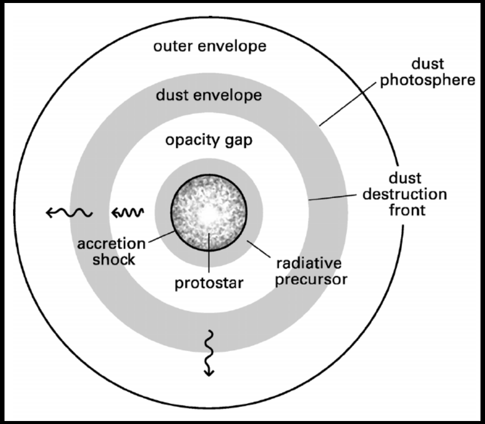

- First core:
  → collapsing dense core becomes opaque in the center
  → chemical composition: mostly H_2
  → not stable: collisional dissociation of H_2 at 2000 K

- Protostar:
  → gains its luminosity from accretion
  → interior described by stellar structure equations
    → first radiative stable, then onset of convection with ignition of D-burning

- Pre-Main Sequence Star:
  → accretion stops
  → gains its luminosity from grav. contraction

- Main sequence star: ignition of H-burning + contraction stops

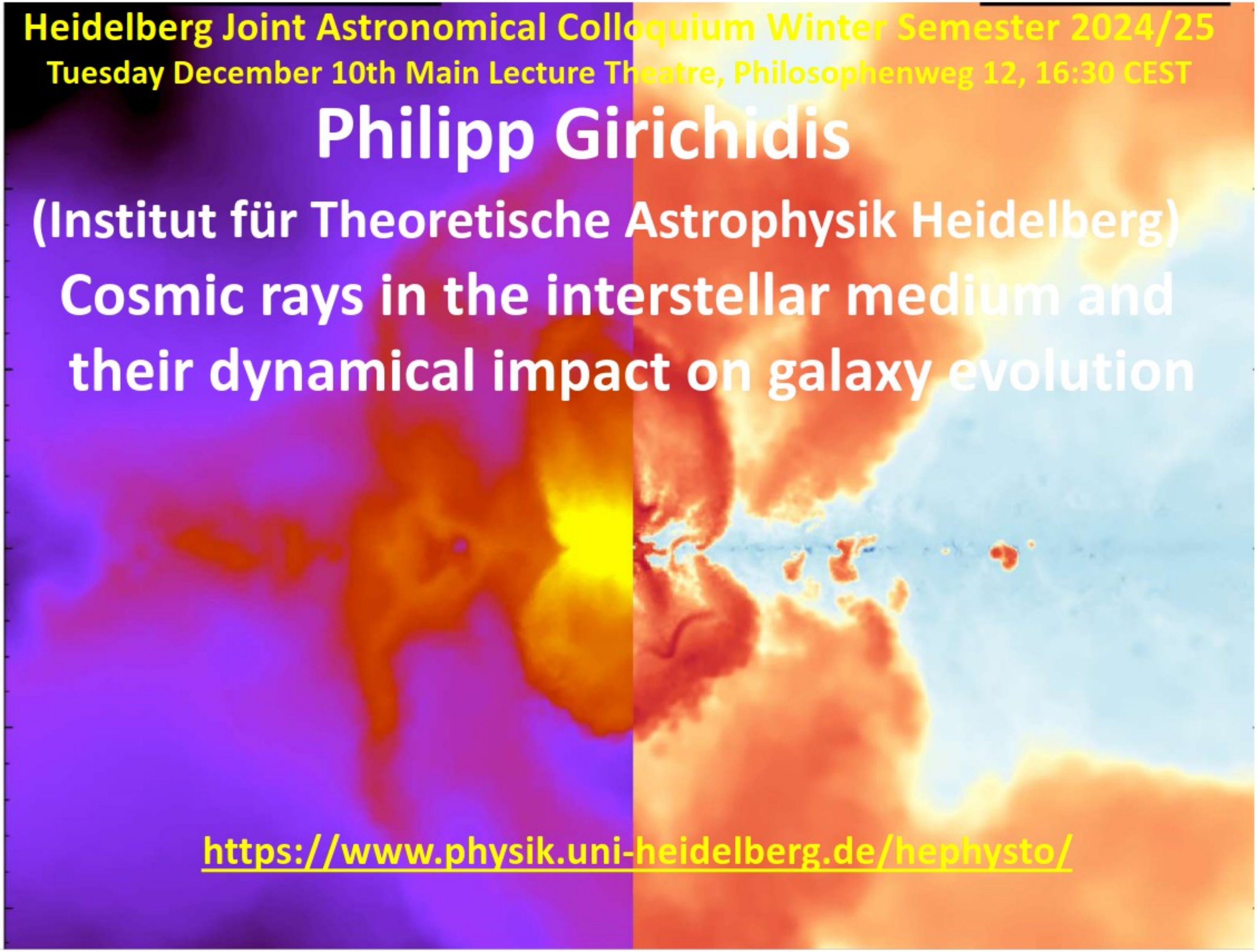
Heidelberg Joint Astronomical Colloquium Winter Semester 2024/25
Tuesday December 10th Main Lecture Theatre, Philosophenweg 12, 16:30 CEST
Philipp Girichidis
(Institut für Theoretische Astrophysik Heidelberg)
Cosmic rays in the interstellar medium and their dynamical impact on galaxy evolution
https://www.physik.uni-heidelberg.de/hephysto/